Reviewed Preprint
v1 • August 21, 2024
Not revised

Reviewed Preprint
v2 • May 12, 2026
Revised by authors

For correspondence:
shenfei_sun@fudan.edu.cn
xlin@fudan.edu.cn

* These authors contributed equally to this work.

Competing interests: No competing interests declared

Funding: See page 24

Reviewing editor: Bernard de Massy, CNRS UM, France

ZNHIT1-dependent H2A.Z deposition at meiotic prophase I underlies pachytene gene expression and meiotic progression during male meiosis

Shenfei Sun[1,2,*], Yamei Jiang[2,*], Ning Jiang[2,*], Qiaoli Zhang[2], Hongjie Pan[3], Fujing Huang[2], Xinna Zhang[1], Yuxuan Guo[1], Xiaoyu You[2], Kai Gong[2], Wei Wei[2], Hanmin Liu[4], Zhenju Song[2], Yuanlin Song[2], Xiaofang Tang[2], Miao Yu[2], Runsheng Li[3], Xinhua Lin[1,2,4]

[1]State Key Laboratory of Reproductive Regulation and Breeding of Grassland Livestock, Institutes of Biomedical Sciences, School of Life Sciences, Inner Mongolia University, Hohhot, China; • [2]State Key Laboratory of Genetic Engineering, Greater Bay Area Institute of Precision Medicine (Guangzhou), School of Life Sciences, Zhongshan Hospital, Fudan University, Shanghai, China; • [3]National Health Commission (NHC) Key Laboratory of Reproduction Regulation, Shanghai Institute for Biomedical and Pharmaceutical Technologies, Shanghai, China; • [4]The Joint Laboratory for Lung Development and Related Diseases of West China Second University Hospital, Sichuan University and School of Life Sciences of Fudan University, Chengdu, China;

eLife Assessment

This study shows that Znhit1, a regulator of chromatin and of the histone variant H2A.Z, is required for progression through meiotic prophase. It is an **important** observation that describes the role of epigenetics and gene expression during meiosis. The analysis is based on complementary approaches at the cytological, single-cell, and genomic levels that provide **solid** evidence for the role of Znhit1 in the control of gene expression and in the loading of H2A.Z in mouse spermatocytes.

https://doi.org/10.7554/eLife.99713.2.sa3

Abstract

Accurate meiotic progression is important for gamete formation and the generation of genetic diversity. However, little is known about the identity of chromatin regulators that underlie mammalian meiosis in vivo. Here, we identify the multifaceted functions of the chromatin remodeler ZNHIT1 in governing meiosis. The expression of *Znhit1* gradually increases during the meiotic prophase, and *Znhit1* knockout in spermatocytes results in arrested pachytene development, impaired DNA double-strand break repair, and defective homologous recombination. Single-cell RNA sequencing and transcriptome analysis reveal that *Znhit1* loss dysregulates meiotic transcriptional programs at the pachytene stage. Chromatin immunoprecipitation data show that ZNHIT1 is needed for the incorporation of the histone variant H2A.Z into pachytene chromatin. Moreover, we found that H2A.Z cooperates with the transcription factor A-MYB to co-bind DNA elements and control gene activity. Our findings provide insights into the regulatory mechanisms governing meiotic progression and highlight ZNHIT1 as a critical regulator of meiotic progression.

Introduction

Meiosis is a fundamental and conserved process that plays a crucial role in gamete formation and the generation of genetic diversity. By undergoing one round of DNA replication and two rounds of cell division, the meiotic process ensures the production of haploid cells, each with a unique combination of genetic materials (Handel and Schimenti, 2010; Lascarez-Lagunas et al., 2020). Any disruptions to the normal progression of meiosis would have significant consequences, such as aneuploidy, infertility, spontaneous abortion, and congenital diseases (Hassold and Hunt, 2001). Therefore, understanding the molecular mechanisms underlying meiosis will provide valuable insights for the diagnosis and treatment of reproductive and developmental diseases.

Multiple chromosomal events occur during meiotic prophase I, including homologous chromosome pairing and synapsis, DNA double-strand break (DSB) formation and repair, and homologous recombination (HR) (Baudat et al., 2013; Hunter, 2015; Zickler and Kleckner, 2023). In this process, homolog pairing and synapsis coincide with SPO11-mediated genome-wide formation of DSBs (Bergerat et al., 1997; Keeney et al., 1997). Following the formation of DSBs, the DNA undergoes resection, leading to the generation of single-stranded DNA overhangs. These overhangs are then coated by RPA, DMC1, and RAD51, facilitating the production of recombination intermediates. Subsequently, these intermediates are processed and resolved, ultimately forming either meiotic crossovers or non-crossovers (Gray and Cohen, 2016; San Filippo et al., 2008; Symington, 2014). The tightly coordinated timing and spatial arrangement of these meiotic events are of utmost importance for proper germ cell development.

There is transcriptional awakening during male meiotic prophase I, in which the meiotic genome becomes transcriptionally active during the zygotene-to-pachytene transition (Alexander et al., 2023; Ernst et al., 2019; Green et al., 2018; Rabbani et al., 2022; Turner, 2015). This process, referred to as pachytene genome activation (PGA) in this context, is responsible for the expression of numerous genes and plays an essential role in controlling meiotic and post-meiotic events. Previous studies have emphasized the significance of the transcription factors (TFs) A-MYB, BRDT, and TCFL5 in activating transcription during pachytene (Alexander et al., 2023; Bolcun-Filas et al., 2011; Cecchini et al., 2023; Gaucher et al., 2012; Li et al., 2013; Maezawa et al., 2020; Manterola et al., 2018; Ozata et al., 2020; Yu et al., 2021). Additionally, extensive chromatin remodeling takes place in spermatocytes during meiotic prophase I, involving histone variant exchange, histone modifications, and high-order genome rearrangement (Kota and Feil, 2010; Wang et al., 2017; Zheng and Xie, 2019). It has been known that SETDB1-mediated H3K9 trimethylation (H3K9me3) is required for sex chromosome transcription silencing (a process called meiotic sex chromosome inactivation, MSCI) and male meiotic procession (Hirota et al., 2018). However, the specific involvement of chromatin regulators in gene activation on autosomes remains poorly understood.

Zinc finger HIT-type containing 1 (ZNHIT1), an evolutionarily conserved subunit of the SRCAP chromatin remodeling complex, acts as a key regulator for the histone variant H2A.Z deposition to control gene expression and cell fate determination (Cai et al., 2005; Cuadrado et al., 2007; Feng et al., 2022). Recent studies have shown that ZNHIT1 is involved in a wide range of developmental processes, including muscle and lens differentiation, heart development, lung branching, and adult tissue stem cell maintenance (Cuadrado et al., 2010; Lu et al., 2022; Sun et al., 2020; Wei et al., 2022; Xu et al., 2021; Zhao et al., 2019). In our previous study, *Znhit1* deletion in early male germ cells impaired the mitosis-to-meiosis transition by regulating *Meiosin* expression (Sun et al., 2022). However, the in vivo function of ZNHIT1 in regulating meiotic progression remains unknown.

To delve into the function of ZNHIT1 in meiosis, we analyzed *Znhit1* expression and observed upregulation specifically during meiotic prophase. Here, we examine the role of ZNHIT1 in multiple meiotic events and show that *Znhit1* deletion in spermatocytes causes defects of pachytene gene expression, thereby resulting in meiotic developmental arrest. Hence, our study highlights the essential role of ZNHIT1 in ensuring meiotic progression.

Results

Znhit1 expression is upregulated during meiotic prophase and *Znhit1* knockout in spermatocytes disrupts spermatogenesis

To identify potential chromatin regulators in meiosis, we first queried for chromatin factors highly expressed during the zygotene stage based on published scRNA-seq data (Fig S1A and Table S1) (Chen et al., 2018). Quantitative analysis showed that the chromatin remodeler *Znhit1* was among the most highly expressed factors (Fig 1A, B, S1B, C). RNA in situ hybridization validated that *Znhit1* expression in male germ cells decreased after meiotic initiation, followed by a gradual increase in spermatocytes from the zygotene stage to the metaphase stage (Fig 1C). These results suggest that ZNHIT1 is a potential chromatin regulator of meiotic progression.

To investigate whether ZNHIT1 regulates meiotic progression, we generated spermatocyte-specific *Znhit1* knockout mice (*Znhit1*$^{fl/fl}$; *Stra8-cre*, referred to as *Znhit1*-sKO). In the first wave of spermatogenesis, Ngn3-negative prospermatogonia directly differentiate into A2 spermatogonia(Law et al., 2019; Rabbani et al., 2022; Yoshida et al., 2006; Yoshida et al., 2004). With Stra8-cre inducing recombination in A1 spermatogonia and preleptotene spermatocytes separately(Lin et al., 2017), it is feasible to generate mice with spermatocyte-specific gene knockout (Fig 1D). RNA in situ experiments on testis sections confirmed the deletion of *Znhit1* mRNA in spermatocytes (Fig 1E, S1D). Compared with littermate controls, *Znhit1*-sKO male mice had smaller testes (Fig S1E, F). PAS-histological and PNA-fluorescent staining illuminated the absence of round spermatids and elongated spermatids in *Znhit1*-sKO testes (Fig 1F, G), indicating that *Znhit1* knockout in spermatocytes disrupted spermatogenesis.

Znhit1 deletion leads to meiotic arrest at the pachytene stage

To study spermatocyte development in *Znhit1*-sKO testes, we co-stained SYCP3, a marker of primary spermatocytes, and HSPA2, a testis-specific HSP70 family member that accumulates from the pachytene stage onward. Both control and *Znhit1*-sKO testis sections exhibited SYCP3^{+}HSPA2^{+} primary spermatocytes (Fig S2A). Phospho-histone H3 (Thr3) (pH3) is a marker of mitotic and meiotic metaphase cells, and *Znhit1* deletion resulted in the complete absence of pH3^{+} metaphase spermatocytes within the seminiferous tubule lumen (Fig S2B). These results suggest that *Znhit1* deletion arrests spermatocytes in meiotic prophase I.

To pinpoint the onset of meiotic failure, we performed immunostaining against SYCP3 in spermatocyte chromosome spreads. The wild-type testes displayed typical spermatocytes at consecutive substages, including leptotene, zygotene, pachytene, diplotene, and diakinesis (Fig 2A). However, spermatocytes at the diplotene and diakinesis stages were rarely observed in *Znhit1*-sKO testes (Fig 2B, C). We also examined the expression of H1T, a middle pachytene marker, and no difference in H1T expression was observed in *Znhit1*$^{-/-}$ spermatocytes (Fig S2C). *Znhit1* knockout resulted in increased TUNEL-positive spermatocytes, suggesting that these defective spermatocytes were eliminated by the apoptotic pathway (Fig 2D, E). We further performed scRNA-seq analysis of postnatal day 35 (P35) testes from control and *Znhit1*-sKO. Uniform manifold approximation and projection (UMAP) showed that germ cells normally progressed through all meiotic stages and successfully gave rise to spermatids in control groups (Fig 2F). By contrast, in the *Znhit1* knockout group, late pachytene spermatocytes decreased significantly, and only very few subsequent germ cell types were observable. *Pou5f2* is expressed explicitly at the diplotene stage, and we found a lack of *Pou5f2*$^{+}$ diplotene spermatocytes in *Znhit1*-sKO testes (Fig 2G). These results indicate that *Znhit1* deletion leads to meiotic arrest at the pachytene stage.

ZNHIT1 is required for DSB repair and meiotic recombination

To investigate the impact of ZNHIT1 on meiotic events, we first performed immunostaining of SYCP1 and SYCP3, the essential components of the synaptonemal complex, to examine whether ZNHIT1 regulates homologous synapses. Pachytene nuclei with fully synapsed autosomes were

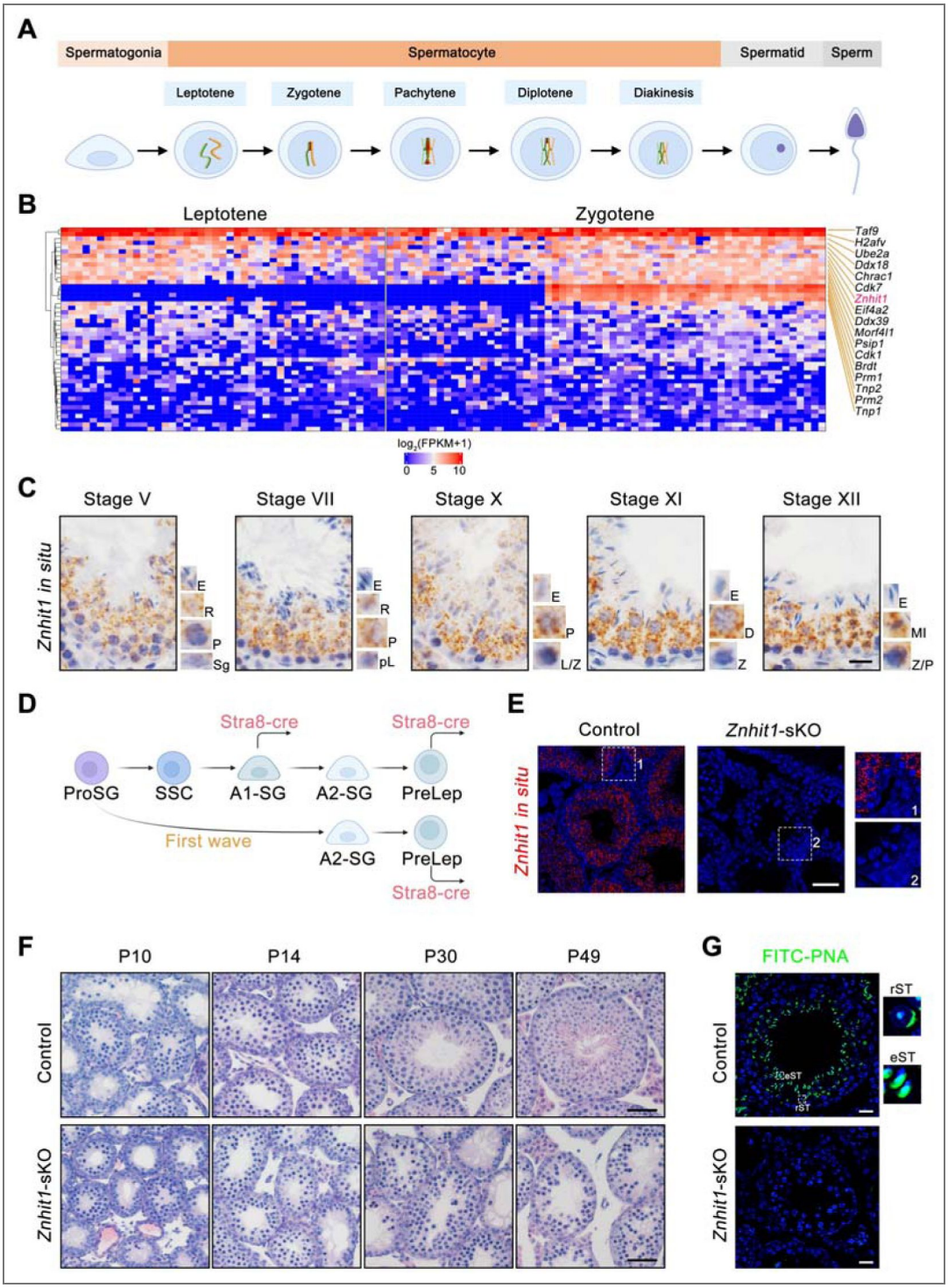

Figure 1. ***Znhit1*** **deletion in spermatocytes disrupts spermatogenesis.**

(**A**) Schematic representation of the male germline development in mice. (**B**) Heatmap showing the clustering of 47 chromatin factors based on the transcription levels in leptotene and zygotene spermatocytes. (**C**) *Znhit1* in situ hybridization in postnatal day 60 (P60) testis sections. Scale bar, 20 μm. Sg, spermatogonia; pL, preleptotene; L, leptotene; Z, zygotene; P, pachytene; D, diplotene; MI, metaphase; R, round spermatids; E, elongating spermatids. (**D**) Schematic diagram showing the onset of Stra8-cre expression in the male germline development. (**E**) *Znhit1* in situ hybridization in P42 testis sections. Scale bar, 50 μm. (**F**) Histological testicular sections in control or *Znhit1*-sKO testis sections at the indicated times. Scale bar, 50 μm. (**G**) Immunostaining of PNA in testis sections from control or *Znhit1*-sKO mice at the indicated times. rST, round spermatids; eST, elongating spermatids. Scale bar, 20 μm. All images are representative of n = 3 mice per genotype.

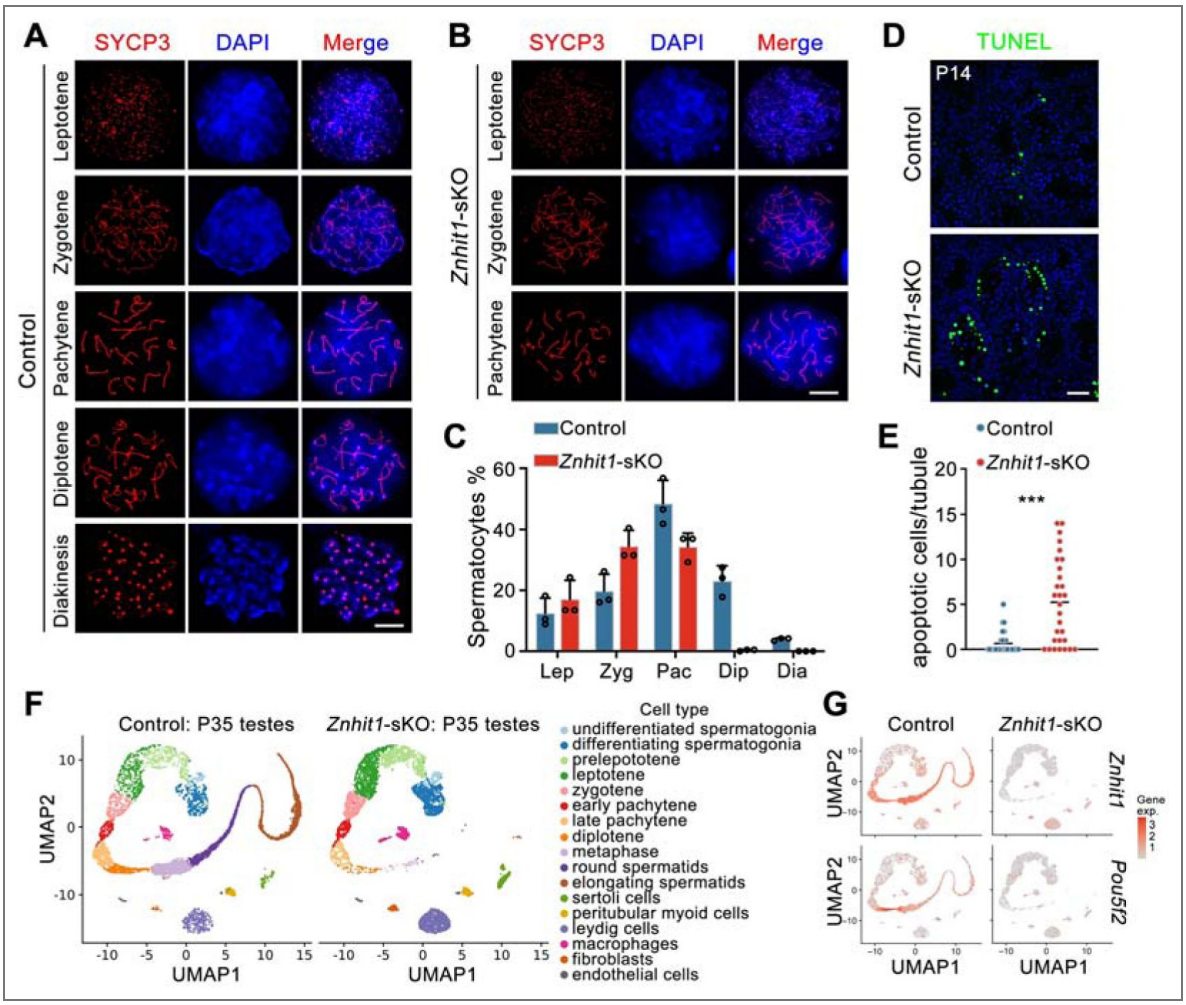

Figure 2. *Znhit1* deletion leads to meiotic pachytene arrest.

(**A-C**) Immunostaining of SYCP3 in spermatocyte chromosome spreads of control (**A**) or *Znhit1*-sKO mice (**B**). Quantitative data are shown in (**C**). Scale bar, 10 μm. (**D** and **E**) TUNEL staining in testis sections from P14 control or *Znhit1*-sKO mice. Quantitative data are shown in (**E**). Scale bar, 40 μm. All images are representative of n = 3 mice per genotype. (**F**) UMAP plot showing the annotated cells captured from P35 control and *Znhit1*-sKO testicular cells. (**G**) UMAP plot showing the expression of *Znhit1* and *Pou5f2* in control P35 control and *Znhit1*-sKO testicular cells. Data are presented as the mean ± s.d. *** $p < 0.001$.

observed in spermatocytes from the control (Fig. 3A). In *Znhit1*-sKO testes, while autosomal synapsis appeared grossly normal, abnormalities were present at the terminal ends of autosomes. During the pachytene stage, the X and Y chromosomes undergo pairing and synapses between the short pseudoautosomal regions (PARs). We found an increase in the percentage of unsynapsed X-Y chromosomes in *Znhit1*-sKO spermatocytes (Fig 3B). Thus, deletion of *Znhit1* results in impaired chromosomal synapsis.

Next, we examined the programmed formation and repair of DSBs by co-staining SYCP3 and γH2AX, a DSB marker, on spermatocyte chromosome spreads. In both control and *Znhit1*-sKO spermatocytes, γH2AX signals were evident in the leptotene and zygotene stages (Fig 3C). However, in *Znhit1*-deficient pachynema, we still observed diffuse γH2AX signals on the autosomes, while in control pachynema, γH2AX signals only accumulated on the X-Y chromosomes. These results demonstrate that ZNHIT1 is required for completing DSB repair.

To understand how ZNHIT1 regulates DSB repair, we performed an immunostaining analysis using the markers RPA2 and RAD51, the essential factors involved in DSB repair. We found an increase in RPA2 and RAD51 counts in both zygonema and pachynema of *Znhit1*-deficient testes (Fig 3D, E, and S3A, B), indicating that *Znhit1* deletion delayed recombinational repair, resulting in defective resolution of autosomal DSBs in *Znhit1*$^{-/-}$ pachynema. The formation and repair of DSBs play crucial roles in initiating and facilitating meiotic recombination, respectively. To examine the consequences of unrepaired DSBs on meiotic recombination in *Znhit1* mutants, we performed an immunostaining analysis against MLH1, a marker of meiotic crossover formation. Indeed, we found an almost absence of MLH1 foci in *Znhit1*$^{-/-}$ pachytene spermatocytes compared with controls (Fig 3F and S3C), indicating that *Znhit1* deletion severely disrupted meiotic crossover formation.

scRNA-seq analysis reveals that *Znhit1* deletion impairs meiotic transcriptional programs

We next investigated whether *Znhit1* deletion impacts meiotic gene expression programs. To address this, we isolated testicular cells from control and *Znhit1*-sKO mice at P16 and performed scRNA-seq analysis. scRNA-seq analysis identified 6 distinct germ cell types based on the expression of canonical stage-specific markers (Chen et al., 2018), including undifferentiated spermatogonia (*Zbtb16*), differentiating spermatogonia (*Kit*), preleptotene spermatocytes (*Nacad*), leptotene spermatocytes (*Meiob*), zygotene spermatocytes (*Psma8*), and pachytene spermatocytes (*Piwil1*) (Fig 4A and S4A, B). We then analyzed the average expression of gene sets dynamically changed during meiotic transitions, including genes upregulated or downregulated at the leptotene-to-preleptotene (Lep/PreL), zygotene-to-leptotene (Zyg/Lep), and pachytene-to-zygotene (Pac/Zyg) stages (Table S2). While *Znhit1* deletion had minimal effects on genes activated or repressed during early meiotic transitions (PreL → Lep and Lep → Zyg), it specifically and severely impaired the transcriptional programs at the zygotene-to-pachytene transition. Specifically, the average expression of 1,560 genes was activated at the pachytene stage (referred to as pachytene-activated genes, or PGA genes), while *Znhit1* deletion downregulated these PGA genes (Fig 4B). Functional enrichment analysis revealed that these PGA genes were primarily involved in DNA repair, cilium organization, and spermatid development, consistent with the biological process of germ cell development (Table S3).

Moreover, we identified differentially expressed genes (DEGs) in each spermatocyte type between the control and *Znhit1*-sKO groups. The number of DEGs gradually increased from the preleptotene to the pachytene stage, with downregulated genes predominating (Fig 4C and Table S4). In particular, *Znhit1*$^{-/-}$ pachytene spermatocytes exhibited 2,785 downregulated genes, among which were most of the pachytene-activated genes (1,094 out of 1,560, 70.1%). Functional enrichment analysis revealed that upregulated genes following *Znhit1* deletion were associated with apoptotic pathways, supporting an observation that *Znhit1* deletion resulted in germ cell clearance through apoptosis (Fig 4D). Moreover, downregulated GO terms included germ cell development and DNA recombination (Fig 4E and Table S5). Interestingly, recent studies showed that cilium organization was essential for spermatocyte development (Mytlis et al., 2022), and

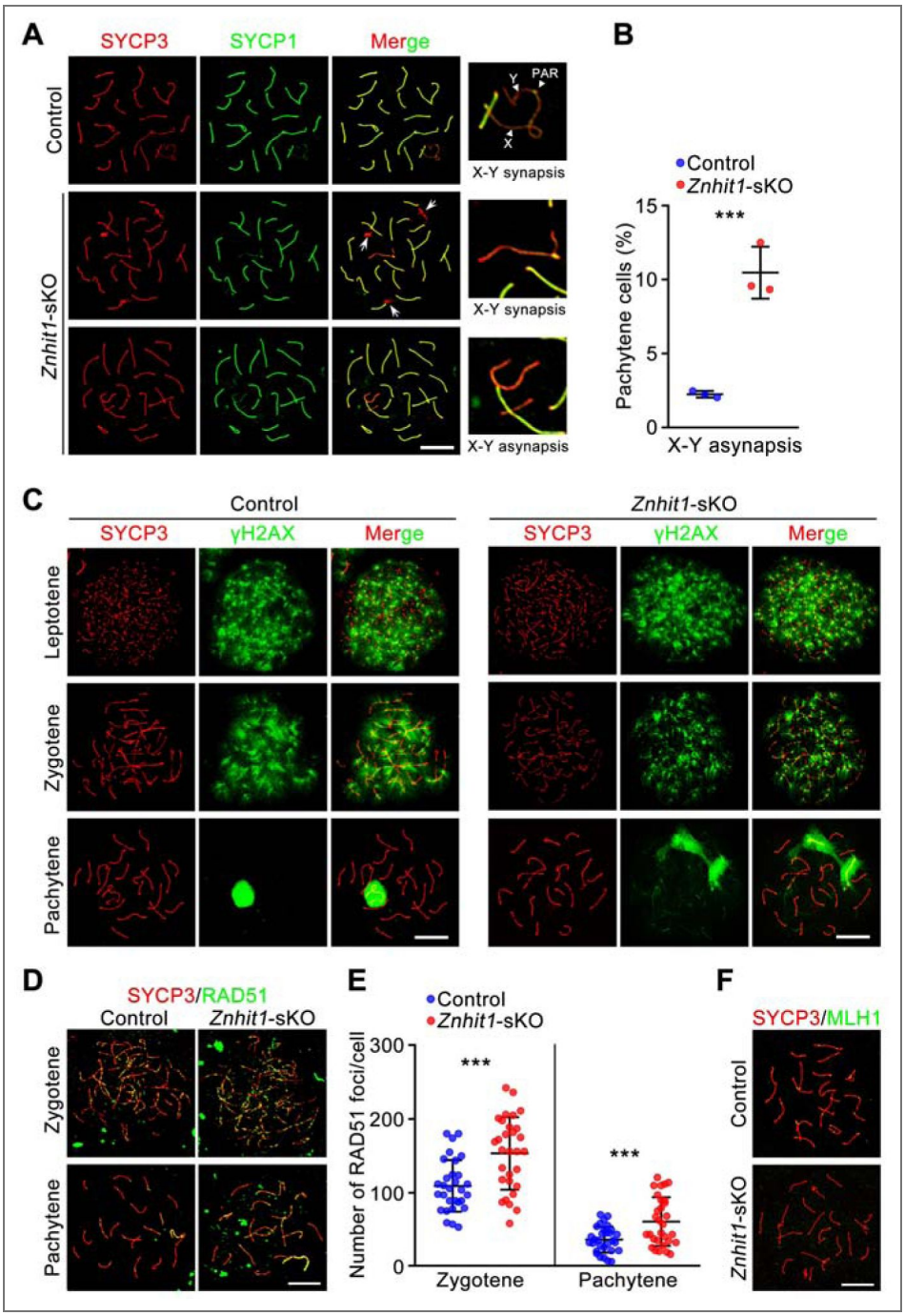

Figure 3. ***Znhit1*** **deletion impairs meiotic recombination.**

(**A** and **B**) Immunostaining of SYCP3 and SYCP1 in spermatocyte chromosome spreads of control or *Znhit1*-sKO mice. Arrows indicate autosomal regions with abnormal synapsis. X, X chromosome; Y, Y chromosome; PAR, pseudoautosomal region. Quantitative data are shown in (**B**). Scale bar, 10 μm. (**C**) Immunostaining of SYCP3 and γH2AX in spermatocyte chromosome spreads of control or *Znhit1*-sKO mice. Scale bar, 10 μm. (**D** and **E**) Immunostaining of SYCP3 and RAD51 in spermatocyte chromosome spreads of control or *Znhit1*-sKO mice. Quantitative data are shown in (**E**). Scale bar, 10 μm. (**F**) Immunostaining of SYCP3 and MLH1 in spermatocyte chromosome spreads of control or *Znhit1*-sKO mice. Scale bar, 10 μm. All images are representative of n = 3 mice per genotype. Data are presented as the mean ± s.d. *** $p < 0.001$.

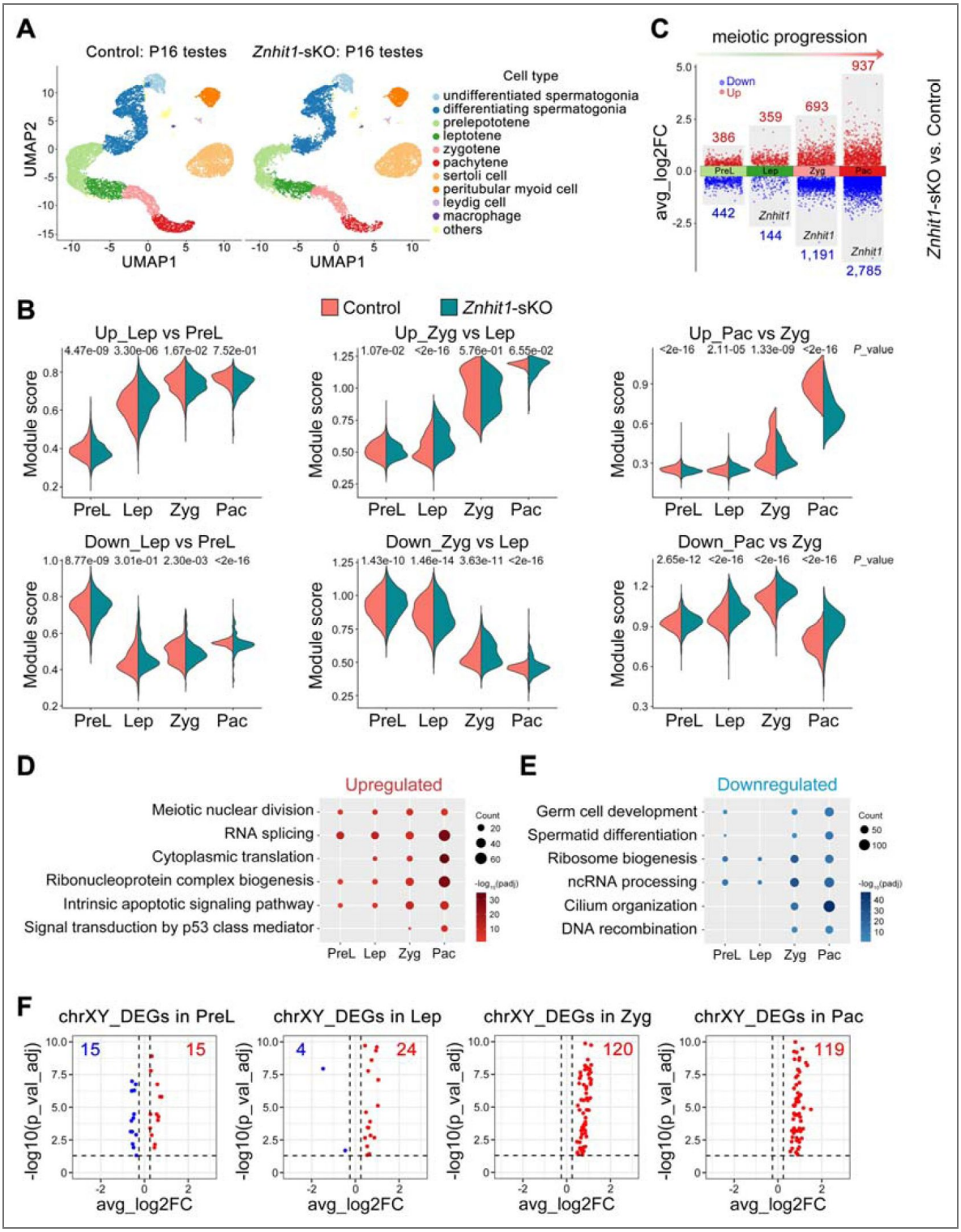

Figure 4. ***Znhit1*** **deletion impairs meiotic transcriptional programs.**

(**A**) UMAP plot showing the annotated cells captured from P16 control and *Znhit1*-sKO testicular cells. (**B**) Violin plots showing the average expression level of upregulated or downregulated genes between two consecutive spermatocyte stages. PreL, preleptotene; Lep, leptotene; Zyg, zygotene; Pac, pachytene. (**C**) Volcano plot showing the distribution of upregulated and downregulated DEGs for each cell type in spermatocytes between control and *Znhit1*-sKO testicular cells. (**D** and **E**) Representative shared Gene Ontology (GO) terms of upregulated and downregulated DEGs at consecutive spermatocyte stages. (**F**) Volcano plot showing differentially expressed XY-linked genes in scRNA-seq data following *Znhit1* deletion.

Znhit1 deletion reduced the expression of cilium-related genes in zygotene and pachytene spermatocytes (Fig 4E). We further conducted bulk RNA-seq experiments with P14 control and *Znhit1*-sKO testicular cells and identified 882 DEGs (812 downregulated genes and 70 upregulated genes) in *Znhit1*-sKO testicular cells (Fig S5A, and Table S6). Through integrative analysis of bulk and single-cell RNA-seq data, we found that the expression of these 812 genes was activated during the zygotene-to-pachytene transition, and *Znhit1* deletion significantly reduced the expression of these genes (Fig S5B). We also analyzed the expression of XY-linked genes. As shown in Figure 4F, while only modest numbers of XY-DEGs were detected at preleptotene and leptotene, a striking accumulation of upregulated XY-DEGs was observed at zygotene (120 genes) and pachytene (119 genes). This aberrant activation of XY-linked genes directly reveals a failure of Meiotic Sex Chromosome Inactivation (MSCI) in *Znhit1*-knockout spermatocytes. Together, these data indicate that ZNHIT1 is essential for the regulation of meiotic transcriptional programs.

Consistent with meiotic recombination defects in *Znhit1* mutants, genes associated with homologous recombination were repressed following *Znhit1* deletion, including *Ccnb1ip1*, *Rnf212*, *Spo16*, *Ankrd31*, and *Terb1* (Boekhout et al., 2019; Papanikos et al., 2019; Qiao et al., 2014; Rao et al., 2017; Reynolds et al., 2013; Shibuya et al., 2014; Wang et al., 2019; Zhang et al., 2019) (Fig S5C, D).

Znhit1 deletion impairs H2A.Z incorporation into pachytene chromatin

We then asked how ZNHIT1 regulates transcription. ZNHIT1 is a subunit of the SRCAP complex that facilitates the incorporation of the histone variant H2A.Z by replacing H2A (Fig S6A)(Yu et al., 2024). Immunostaining against H2A.Z showed a gradual increase in H2A.Z accumulation on autosomes from the leptotene to the diakinesis stage, while the H2A.Z signal was markedly low on the X-Y body (Fig 5A). *Znhit1* loss decreased H2A.Z staining on the pachytene cells, suggesting that ZNHIT1 is required for maintaining H2A.Z integrity during meiosis.

To profile H2A.Z target genes, we performed chromatin immunoprecipitation followed by sequencing (ChIP-seq) against H2A.Z in P14 testicular cells. Using the ChromHMM model to annotate H2A.Z signals with meiocyte chromatin states defined by published epigenetic markers (Spruce et al., 2020), we found that H2A.Z sites were primarily enriched in chromatin state 1 and state 2 (promoters and enhancers) but were less enriched in recombination hotspots (Fig 5B, C), consistent with previously published results (Spruce et al., 2020). Quantitative analysis showed significant H2A.Z reduction at 37.9% (23,926 of 63,109) of H2A.Z-bound genome sites following *Znhit1* deletion (Fig 5D). Comparison analysis with bulk RNA-seq data identified 480 downregulated DEGs with decreased H2A.Z signals (Fig 5E). ~41.3 and 37.8% of the downregulated H2A.Z peaks occupied promoters and enhancers, respectively. At promoters, these downregulated H2A.Z preferentially occupied active promoters (H3K4me3 only), while H2A.Z occupied three types of enhancers: active, poised, and primed enhancers (Fig 5F, and S6B, C). These findings indicate that *Znhit1* deletion impairs H2A.Z incorporation into pachytene chromatin.

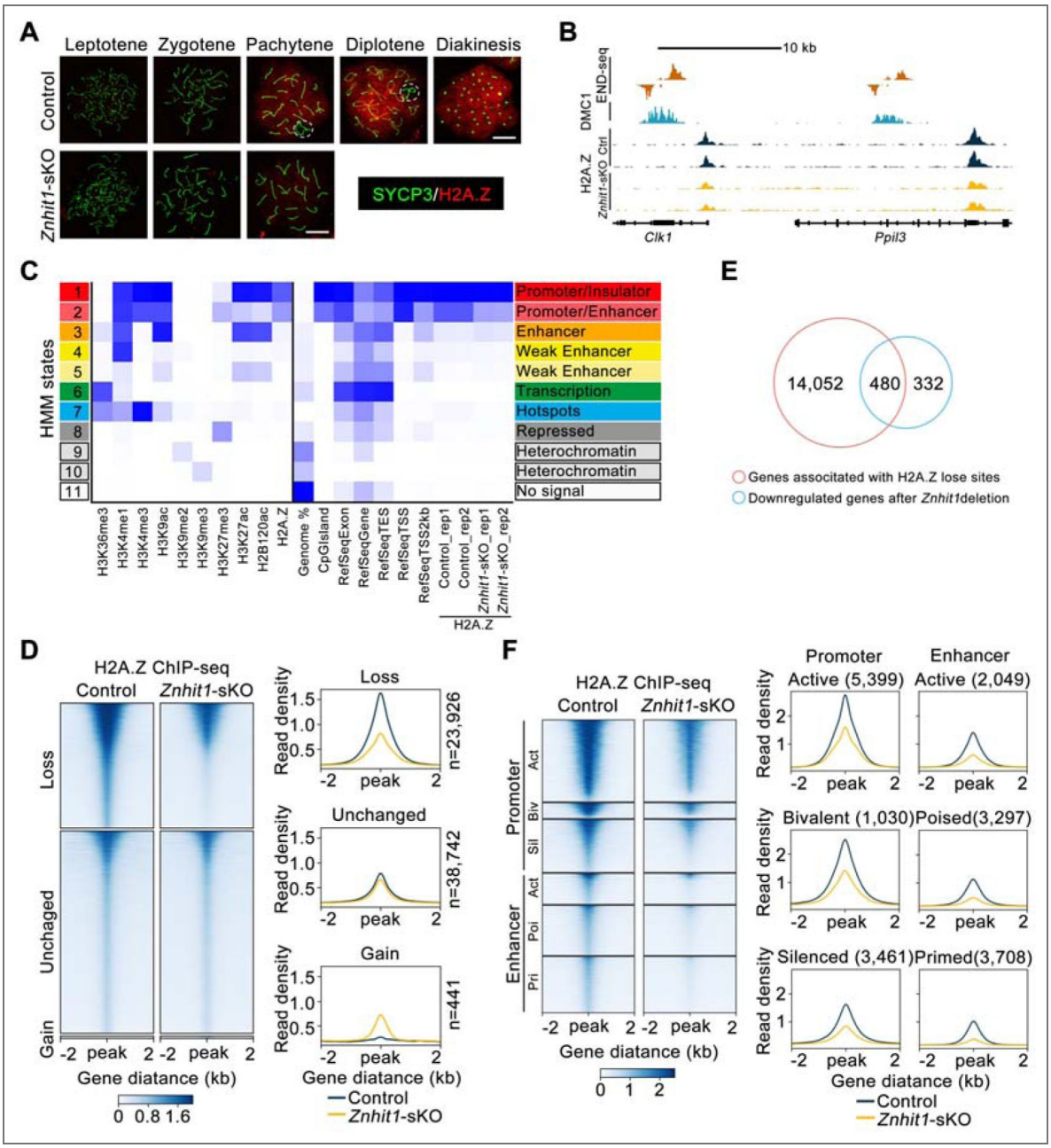

Figure 5. ZNHIT1 regulates H2A.Z binding on promoter and enhancer regions.

(**A**) Immunostaining of SYCP3 and H2A.Z in spermatocyte chromosome spreads of control or *Znhit1*-sKO mice. The dashed circle indicates X-Y chromosomes. Scale bar, 10 μm. (**B**) Representative tracks of END-seq, DMC1-SSDS, and H2A.Z ChIP-seq in wild-type, control, or *Znhit1*-sKO testicular cells. (**C**) Heatmaps of chromatin states produced by ChromHMM and showing different enrichment for H2A.Z in control or *Znhit1*-sKO testicular cells. (**D**) Heatmaps and mean plots of H2A.Z ChIP-seq signal in control or *Znhit1*-sKO testicular cells (n = 2). (**E**) Venn diagram showing the overlap between decreased H2A.Z-bound genes and downregulated genes in *Znhit1*-sKO testicular cells. (**F**) Heatmaps and mean plots of downregulated H2A.Z ChIP-seq signals surrounding different types of promoters and enhancers.

H2A.Z deposition cooperates with A-MYB to regulate transcription

We further asked how ZNHIT1/H2A.Z deposition facilitates lineage-specific gene expression. We performed TF motif analysis using active promoters/enhancers with decreased H2A.Z signals. This analysis identified several MYB family TFs, including MYB, A-MYB, and B-MYB (Fig 6A). Gene regulatory network analysis conducted by SCENIC further identified A-MYB (encoded by the *Mybl1* gene) as the core regulatory TF in spermatocytes (Fig 6B). We reanalyzed RNA-seq data in P14 testes from A-MYB-deficient mice (Li et al., 2013) and found that A-MYB-deficient DEGs correlated with those observed in *Znhit1*-deficient testicular cells (Fig 6C). Although *Znhit1* deletion didn't affect *Mybl1* mRNA expression, transcriptome analyses showed that the expression of A-MYB target genes was significantly reduced in *Znhit1*$^{-/-}$ pachytene spermatocytes (Fig 6D, E, and S7A). These results suggest that *Znhit1*$^{-/-}$ and *Mybl1*$^{-/-}$ pachytene spermatocytes share common gene expression alterations.

Next, we compared the genome binding sites of H2A.Z and A-MYB. Utilizing published A-MYB ChIP-seq data from P14 testicular cells (Li et al., 2013), we identified 6,088 A-MYB binding signals, with 78.1% (4755) of these coinciding with H2A.Z peaks (Fig 6F). Annotation of genomic features showed that approximately 66.52% and 12.02% of these overlapping sites occupied active promoters and enhancers, respectively, representing a stronger enrichment compared to other regulatory elements (Fig 6G). Genes associated with H2A.Z and A-MYB binding included essential HR-related genes, such as *Ccnb1ip1* (Fig 6H). Moreover, we showed that *Znhit1* deletion resulted in a marked reduction in H2A.Z signals and nascent transcription identified by KAS-seq signals (Fig 6I). We further linked KASDseq signals with gene expression profiles, and found that *Znhit1* depletion caused a global reduction in KASDseq signals, especially at promoters of downregulated genes (Fig S8A), indicating defective transcription bubble formation. In comparison, genes with increased expression showed low KASDseq signals in both control and mutant groups, likely reflecting indirect regulation. These results further support the essential role of ZNHIT1 in transcriptional regulation.

Previous studies have shown the fundamental role of A-MYB in activating meiotic enhancers (Maezawa et al., 2020). We found that *Znhit1* deletion resulted in reduced KAS-seq signals at active enhancers (Fig 6I). Interestingly, the chromatin accessibility detected by ATAC-seq at active enhancers increased after *Znhit1* deletion, suggesting that *Znhit1* deletion results in dysregulated chromatin state. These findings suggest that ZNHIT1/H2A.Z deposition is essential for enhancer activation.

Together, these results demonstrate the critical role of the ZNHIT1/H2A.Z/A-MYB axis in governing meiotic transcriptional programs.

Discussion

Meiosis plays a crucial role in the production of haploid gametes. Any disturbances during meiotic progress are known to lead to infertility and congenital diseases. Here we delineate the multifaceted functions of the chromatin remodeler ZNHIT1 in regulating meiotic progression. Our study provides convincing data to show that the ZNHIT1/H2A.Z/A-MYB axis controls spermatocyte development, meiotic recombination, and PGA. Thus, these findings underscore the significance of specific chromatin structures in governing appropriate transcriptional reprogramming and precise meiotic progression.

The role of H2A.Z in DNA injury and repair has been extensively studied (Colino-Sanguino et al., 2022; Dong et al., 2014; Xu et al., 2012; Yamada et al., 2018), but its function in programmed DSB formation and repair during mammalian meiosis remains unknown. To address this question, we generated *Znhit1* conditional knockout mice specifically during male meiosis to examine the role of ZNHIT1-mediated H2A.Z deposition in the formation and repair of programmed DSB. One new observation in this study is that *Znhit1* loss is dispensable for DSB formation but necessary for DNA break repair during meiosis. Intriguingly, unlike the observations in plant meiosis but consistent with Christopher L. Baker's group observation in

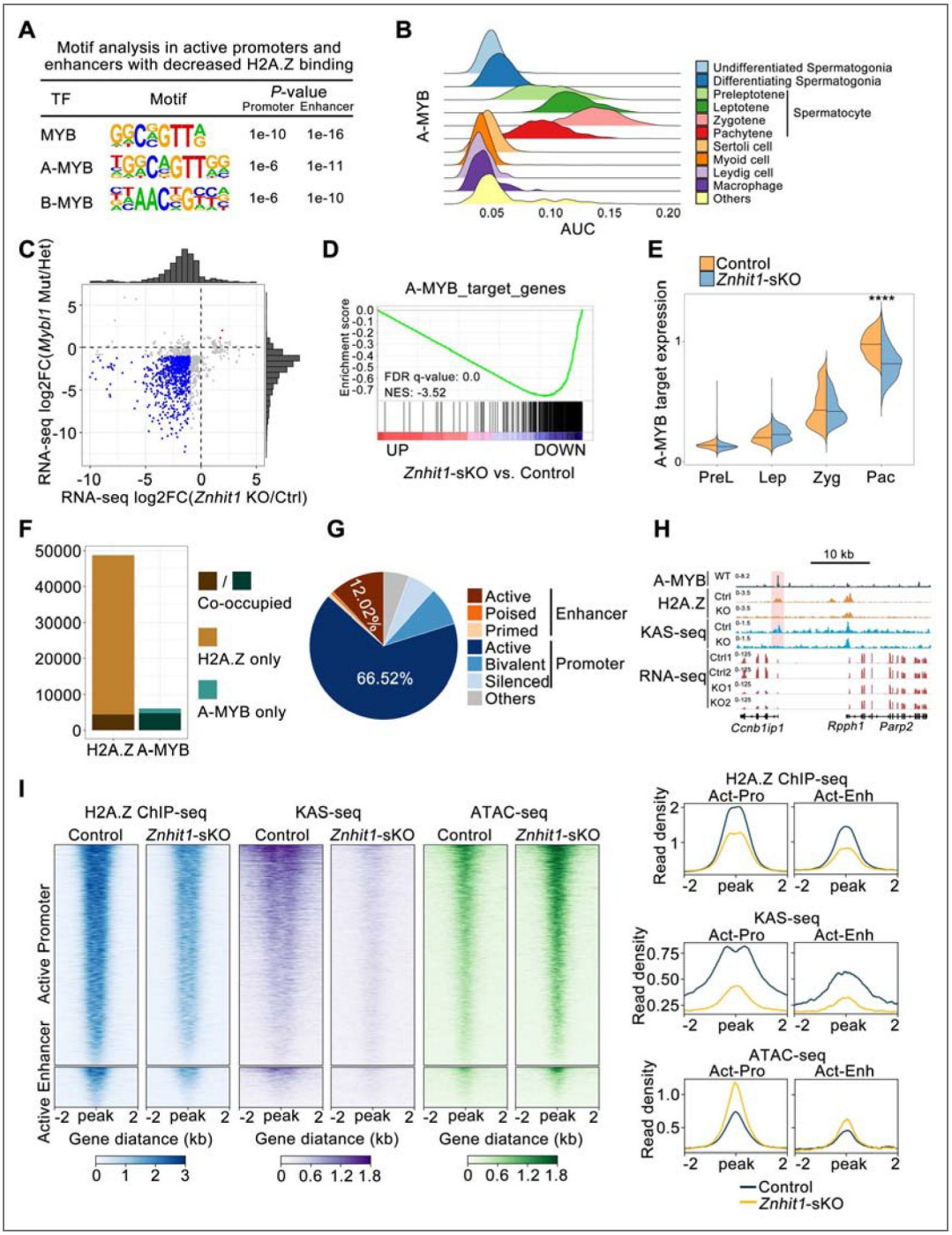

Figure 6. ZNHIT1/H2A.Z/A-MYB axis regulates chromatin state and gene expression.

(**A**) Motif analysis of active promoters or active enhancers with decreased H2A.Z binding for putative transcription factor (TF)-binding sites using the HOMER database. (**B**) Ridge map showing the A-MYB activity (AUC) at each cell type. (**C**) Scatter plot with marginal histograms comparing the fold change of DEGs from *Mybl1*-related RNA-seq data with *Znhit1*-related RNA-seq data in P14 testicular cells. (**D**) GSEA of RNA-seq data for the control and *Znhit1*-sKO testicular cells. Selected gene sets encoded products related to A-MYB target genes. (**E**) Violin plots showing the expression of A-MYB target genes at consecutive spermatocyte stages. (**F**) Histogram showing H2A.Z and A-MYB binding sites. (**G**) Pie chart showing the distribution of H2A.Z and A-MYB co-binding sites. (**H**) Representative H2A.Z ChIP-seq tracks, KAS-seq signals, and RNA-seq signals of the *Ccnb1ip1* locus in the control and *Znhit1*-sKO testicular cells, compared with A-MYB ChIP-seq peaks. (**I**) Heatmaps and mean plots of H2A.Z ChIP-seq, KAS-seq, and ATAC-seq showing signal changes within A-MYB and H2A.Z co-binding active promoters or active enhancers. ******** $p < 0.0001$.

mouse, we confirmed that H2A.Z does not directly bind DNA recombination sites in mammalian spermatocytes (Choi et al., 2013; Spruce et al., 2020; Wang and Copenhaver, 2018). Moreover, we showed that *Znhit1* deletion delays recombinational repair but has limited impacts on DNA resection, ultimately causing defective meiotic crossover formation. Importantly, our study demonstrates that ZNHIT1 is essential for the expression of meiotic recombination-related genes, such as *Ccnb1ip1* and *Rnf212*, implying that ZNHIT1/H2A.Z modulates meiotic recombination through transcriptional regulation, rather than a direct regulatory effect of ZNHIT1 on recombination machinery. Therefore, our data reveal a different mechanism underlying meiotic recombination between plants and mammals.

Pachytene spermatocytes utilize a highly specific mechanism of meiotic surveillance, the pachytene checkpoint, to prevent aneuploidy formation by removing abnormal germ cells with incomplete chromosome synapsis and defective homologous recombination (Huang and Roig, 2023; Roeder and Bailis, 2000; Subramanian and Hochwagen, 2014). Two checkpoint pathways exist in male meiosis: one responding to unrepaired DSBs and the other triggered by MSCI failure (Royo et al., 2013). However, whether epigenetic regulation is involved in meiotic surveillance is not well defined. Previous studies have reported that upon stimulation by unrepaired DSBs, the MRE11-ATM-CHK2 pathway is activated to eliminate aberrant germ cells (Marcet-Ortega et al., 2017). Our study found that *Znhit1* deletion impairs pachytene development and XY-linked gene repression, ultimately causing meiotic pachytene arrest and apoptosis. Therefore, these findings demonstrate that ZNHIT1 acts as an important chromatin factor involved in the regulation of the pachytene checkpoint.

It has long been noticed that in meiotic prophase I, chromatin that has not yet completed chromosomal synapses is transcriptionally inactive, known as meiotic silencing of unsynapsed chromatin (MSUC) (Turner et al., 2005). When germ cells enter the pachytene stage, a large number of protein-coding genes and non-coding RNAs begin to be actively expressed, known as PGA. Previous studies have shown that transcription factors A-MYB and BRDT are involved in transcriptional activation during meiotic prophase, but how PGA takes place in the chromatin context is unclear. In this study, we found that the expression of the chromatin remodeler Znhit1 is specifically upregulated during the zygotene-to-pachytene transition. We also observed that H2A.Z deposition is enriched in the autosomes but less in the sex chromosomes at the pachytene stage. *Znhit1* deletion in spermatocytes repressed pachytene gene activation globally and reduced chromosome-wide H2A.Z deposition, supporting a central role of ZNHIT1 in PGA regulation and chromatin remodeling. It has been known that A-MYB is a transcription factor that controls pachytene transcription activation. We found that *Znhit1*-deficient spermatocytes phenocopied abnormal meiotic phenotypes observed in A-MYB mutants, such as X-Y synapsis failure, impaired DSB repair, and defective HR (Alexander et al., 2023; Bolcun-Filas et al., 2011; Li et al., 2013; Maezawa et al., 2020). Our results also revealed that ZNHIT1/H2A.Z cooperates with A-MYB to regulate PGA gene activation. Therefore, our study illuminates the molecular mechanisms underlying the fundamental question of how PGA is regulated.

The histone variant H2A.Z is enriched at gene promoters and regulatory regions, yet there is ongoing debate about its role in transcriptional regulation. A recent paper reported that H2A.Z knockout in post-mitotic muscle cells has limited effects on gene expression (Belotti et al., 2020). In this study, we utilized the meiotic prophase as a model system (where DNA replication does not occur) to study H2A.Z's function in transcriptional regulation. We found that ZNHIT1-mediated H2A.Z deposition, independent of DNA replication, is indispensable for the transcriptional activation of a large number of meiotic genes. One explanation of this conflicting phenomenon is that H2A.Z dynamics, but not stable H2A.Z accumulation is essential for priming transcriptional changes.

Through the integration of functional and molecular evidence, our findings establish the critical involvement of ZNHIT1-dependent chromatin remodeling in the orchestration of meiotic progression and coordination of various meiotic processes, such as HR and PGA. Furthermore, we

pinpoint the pivotal role played by the ZNHIT1/H2A.Z/A-MYB axis in driving transcriptional reprogramming during meiotic prophase. Taken together, this study deepens our understanding of the interplay between epigenetic regulation and mammalian meiosis.

Materials and Methods

Animals

Znhit1$^{fl/fl}$ mice have been previously described (Zhao et al., 2019) and are available from the Model Animal Research Center of Nanjing University (MARC, Nanjing, China). The *Stra8-cre* knock-in mouse line was kindly provided by Dr. Ming-Han Tong(Lin et al., 2017). All mice were maintained on the C57BL/6J background. Germ cell-specific *Znhit1* knockout mice (*Znhit1*$^{fl/fl}$; *Stra8-cre*) were obtained by crossing *Znhit1*$^{fl/+}$; *Stra8-cre* mice with *Znhit1*$^{fl/fl}$ mice. All mice were housed in the SPF (Specific-Pathogen-Free) animal facility with standard 12 h light/dark cycles and standard temperature (22 to 24D). All mice were provided with ad libitum access to standard laboratory food and water. All experiments in this study were performed following relevant guidelines and approved by the Animal Care and Use Committee of Fudan University.

Histological and immunohistochemical analysis

Testes were fixed in modified Davidson's fixative as previously described (Latendresse et al., 2002), embedded in paraffin, and sectioned. For periodic acid-Schiff (PAS)-hematoxylin staining, 5 μm testis sections were deparaffinized, rehydrated, and stained with Schiff's reagent and hematoxylin solution. For immunofluorescent staining, 5 μm testis sections were retrieved by sodium citrate antigen retrieval buffer (pH 6.0) and blocked with 5% BSA in PBS for 30 min at room temperature. The sections were later incubated overnight at 4°C with primary antibodies as follows: mouse anti-SYCP3 (Abcam, ab97672), rabbit anti-HSPA2 (Abcam, ab108416), rabbit anti-pH3 (Millipore, H0412), rabbit anti-H1T (Invitrogen, PA5-51200), or lectin PNA (SigmaDAldrich, L7381). On the following day, secondary fluorescein-conjugated antibodies and DAPI (SigmaDAldrich, D9542) were added for 1 h, followed by Fluoromount-G mounting (Southern Biotech, 0100-01). Images were analyzed using the confocal microscope.

TUNEL staining was carried out using the DeadEnd^{TM} Fluorometric TUNEL System (Promega, G3250) according to the manufacturer's instructions.

Immunostaining of spermatocyte chromosome spreads

Spermatocyte chromosome spreads were prepared as previously described (Alavattam et al., 2018). Briefly, the clumps of seminiferous tubules were transferred to the hypotonic extraction buffer (30 mM Tris base, 17 mM trisodium citrate, 5 mM EDTA, 50 mM sucrose, 5 mM dithiothreitol (DTT), and 1× protease inhibitor, pH 8.2) and incubated on ice for 1.5 h. The clumps of tubules were then transferred to 30 μL of ice-cold 100 mM sucrose and mashed gently using tweezers to obtain a cell suspension. An additional 30 μL of ice-cold 100 mM sucrose was added to the cell suspension and mixed several times. Positively charged slides were incubated in the ice-cold fixation solution (2% paraformaldehyde, 0.1% Triton X-100, and 0.02% SDS, pH 9.2) for 3 min. 30 μL of the diluted cell suspension was applied to the slides and incubated in humid chambers at room temperature for 2 h. The slides were washed with 0.4% Photo-Flo 200 and stored at −80D.

For immunostaining of spermatocyte chromosome spreads, slides were washed with PBS and blocked with 5% BSA in PBS for 30 min at room temperature. The slides were stained with primary antibodies as follows: rabbit anti-SYCP3 (Abcam, ab15093), mouse anti-SYCP3 (Abcam, ab97672), rabbit anti-SYCP1 (Abcam, ab15090), mouse anti-γH2AX (BioLegend, 613401), rabbit anti-RAD51 (Proteintech, 14961-1-AP), rabbit anti-RPA2 (Proteintech, 10412-1-AP), rabbit anti-MLH1 (Cell Signaling Technology, 3515T), rabbit anti-H2A.Z (Abcam, ab4174).

Znhit1 in situ hybridization

Testis sections (5 μM) at the indicated times were prepared for *Znhit1* in situ hybridization with the RNAscope kit (Advanced Cell Diagnostics, 323100) according to the manufacturer's instructions.

Quantitative reverse transcription PCR (RT-qPCR)

Total RNA was isolated using the RNeasy Mini-plus Kit (Qiagen, 74134) and then reverse-transcribed into complementary DNA (cDNA) with the GoScript Reverse Transcription System (Promega, A5003). cDNA was used as the template for the quantitative PCR assay using 2×SYBR Green qPCR Master Mix (Bimake, B21202). Quantitative PCR primers are listed in Table S7.

RNA-seq library generation and sequencing

Total RNA from fresh testes was isolated and mRNA was purified with magnetic beads (Vazyme, N401-01). Then, mRNA was fragmented and processed to generate RNA-seq libraries (Vazyme, NR605-01). Over 40 million reads were obtained per sample using the Illumina NovaSeq platform for 2 independent biological replicates.

Single-cell RNA sequencing (scRNA-seq)

P16 and P35 control and *Znhit1*-sKO testes were digested by collagenase IV and trypsin at 37D for 10 min to obtain testicular cell suspensions. scRNA-seq libraries were constructed using a 10x Genomics kit and sequenced on the Illumina platform.

ChIP-seq library generation and sequencing

ChIP-seq library generation was performed as previously described. Briefly, P14 control and *Znhit1*-sKO testes were digested by collagenase IV and trypsin at 37D for 10 min, crosslinked with 1% formaldehyde for 10 min, and quenched with glycine. The cells were lysed and sheared with a Bioruptor Plus machine for 20 min. Then, 2 μg of anti-H2A.Z antibody (Abcam, ab4174) was added to the sonicated chromatin and incubated overnight at 4D. The following day, 20 μL of protein G beads were added and incubated for 2 h at 4D. The beads were washed and reverse-crosslinked for 4 h at 65D. DNA was extracted using phenol-chloroform and subjected to library construction using the VAHTS Universal DNA Library Prep Kit for Illumina (Vazyme, ND607-01) according to the manufacturer's instructions. Over 30 million reads were obtained per sample using the Illumina NovaSeq platform for 2 independent biological replicates.

KAS-seq library and ATAC-seq library generation and sequencing

Testes were digested by collagenase IV and trypsin at 37D for 10 min. Pachytene cells were sorted using fluorescence-activated cell sorting (FACS) as previously described (Long et al., 2017). For KAS-seq, pachytene cells were labeled with N3-kethoxal, and DNA was isolated using the DNA Clean and Concentrator kit (Zymo, D4013) and subjected to library construction using Q5 high-fidelity DNA polymerase (New England Biolabs, M0544S). Genomic DNA was fragmented using Tn5 transposase and subjected to library construction. For ATAC-seq, pachytene nuclei were isolated and fragmented with Tn5 transposase. DNA was isolated using the DNA Clean and Concentrator kit (Zymo, D4013) and subjected to library construction using Q5 high-fidelity DNA polymerase (New England Biolabs, M0544S). For high-throughput sequencing, over 30 million reads were obtained per sample using the Illumina NovaSeq platform for 2 independent biological replicates.

RNA-seq data analysis

We performed RNA-seq analysis as described previously (Pertea et al., 2016). Briefly, after removing adapters using Cutadapt (v2.5) (Kechin et al., 2017), paired-end reads were aligned to the annotated mouse transcripts (mm10 Gencode vM23 release) using Hisat2 (v2.2.1) (Kim et al., 2015; Kim et al., 2019). Gene expression levels were calculated using StringTie (v2.2.1) (Pertea et al., 2015). Read counts were calculated using a Python script (prepDE.py3) provided by the

StringTie development team. Differentially expressed genes were identified using the R package DESeq2 (v1.38.3) (Love et al., 2014). Genes with read counts > 50 in at least one sample were kept for further analysis. A given gene was considered to significantly changed if the adjusted P value (padj) was < 0.05, the P value was < 0.01, and the fold-change was≥ 2. Gene Set Enrichment Analysis (GSEA) was carried out using GSEA software (Subramanian et al., 2005). GO analysis was performed using clusterProfiler (v4.6.2) (Wu et al., 2021).

scRNA-seq data analysis

FASTQ files were run through CellRanger (v7.1.0) software with default parameters for de-multiplexing, aligning reads with STAR software to mm10, and counting unique molecular identifiers (UMIs). As input files of the Seurat R package (v4.4.0), the filtered gene expression matrices were then used for downstream analyses (Butler et al., 2018). Low-quality cells were filtered (expressing < 500 or >6,000 unique gene counts and >15% mitochondrial reads). Principal component analysis was performed on SCT-transformed data using 3,000 variable genes. The top 50 principal components were used for clustering and visualized using the UMAP algorithm in the Seurat R package. The "FindAllMarkers" function of the Seurat R package was used to calculate cluster-specific genes. Marker genes for each cluster are shown in Table S8.

The "FindMarkers" function of the Seurat R package was used to identify differentially expressed genes (DEGs) for spermatocytes (preleptotene, leptotene, zygotene, and pachytene). Only those with |'avg_logFC'| > 0.25 and 'p_val_adj' < 0.05 were considered as DEGs. For the transcriptional regulatory network analysis, the raw count matrix was used by the pyscenic (v0.12.1) workflow using default parameters (Aibar et al., 2017). Then, the output loom file was opened by the SCENIC R package (v1.3.1), and AUC values of regulons were extracted for visualization of downstream transcription factor activity.

ChIP-seq and KAS-seq data analysis

For analyzing ChIP-seq and KAS-seq data, we used the ENCODE ChIP-seq pipeline (v2.2.1, *https://github.com/ENCODE-DCC/chip-seq-pipeline2*). Raw reads were cleaned by Cutadapt (v2.5) (Kechin et al., 2017). After removing adapters, clean reads were aligned against the mouse mm10 genome using bwa (v0.7.17) (Li and Durbin, 2009). Then, sam files were converted to bam files using samtools (v1.9) (Li et al., 2009). PCR duplicates were removed using Picard (v2.20.7) (*https://broadinstitute.github.io/picard/*). Histone ChIP-seq peaks (such as H2A.Z and histone marks) and KAS-seq peaks were called using MACS2 (v2.2.4) (Zhang et al., 2008), while transcription factor ChIP-seq peaks (such as A-MYB) were called using the R packages spp (v1.15.5) (*https://github.com/hms-dbmi/spp*). The conservative narrow peaks were used for downstream analysis.

For visualization, bam files were converted to bigWig files using deepTools (v3.3.1) (Ramirez et al., 2014), and bigWig files were used to calculate tag density under 50 bp resolution. In addition, CPM was used to normalize the number of reads per bin. We used the R package DiffBind (v3.8.4) (*http://bioconductor.org/packages/release/bioc/html/DiffBind.html*) for differential peak analysis and the R package rGREAT (v2.1.11) (Gu and Hubschmann, 2023) for peak annotation. We used ComputeMatrix and plotHeatmap of deepTools to generate count matrices and heatmaps, respectively. H2A.Z enrichment within chromatin states was annotated using the ChromHMM model (Ernst and Kellis, 2012; Spruce et al., 2020). TF motif enrichment was calculated using HOMER (v4.11) (Heinz et al., 2010). We used deepTools to draw Pearson's correlation scatter plots for the correlation between replicates of each experiment.

For promoter and enhancer type analysis, H3K27ac ChIP-seq data in wild-type pachytene spermatocytes were downloaded from the published data (GSE107398) (Adams et al., 2018); ChIP-seq data for H3K4me1, H3K4me3, and H3K27me3 in wild-type pachytene spermatocytes were downloaded from the published data (GSE132446) (Chen et al., 2020).

ATAC-seq data analysis

ATAC-seq data were analyzed using a standardized ENCODE ATAC-seq pipeline (v2.2.2, *https://github.com/ENCODE-DCC/atac-seq-pipeline*). The mouse reference genome (mm10) was used in the pipeline. Trimming, mapping, and duplicate-removing were performed as the ENCODE pipeline suggested using Cutadapt (v2.5) (Kechin et al., 2017), Bowtie2 (v2.3.4.3) (Langmead et al., 2009), and Picard (v2.20.7) (*https://broadinstitute.github.io/picard/*) respectively. MACS2 (v2.2.4) (Zhang et al., 2008) was used for peak calling.

Statistics and reproducibility

Statistical analyses were performed using R and Prism 9. Data are presented as means ± s.d. unless otherwise indicated. The two-tailed, unpaired, Student's t-test, Mann–Whitney test, or one-way or two-way ANOVA were performed to analyze statistical significance.

Supplementary Materials

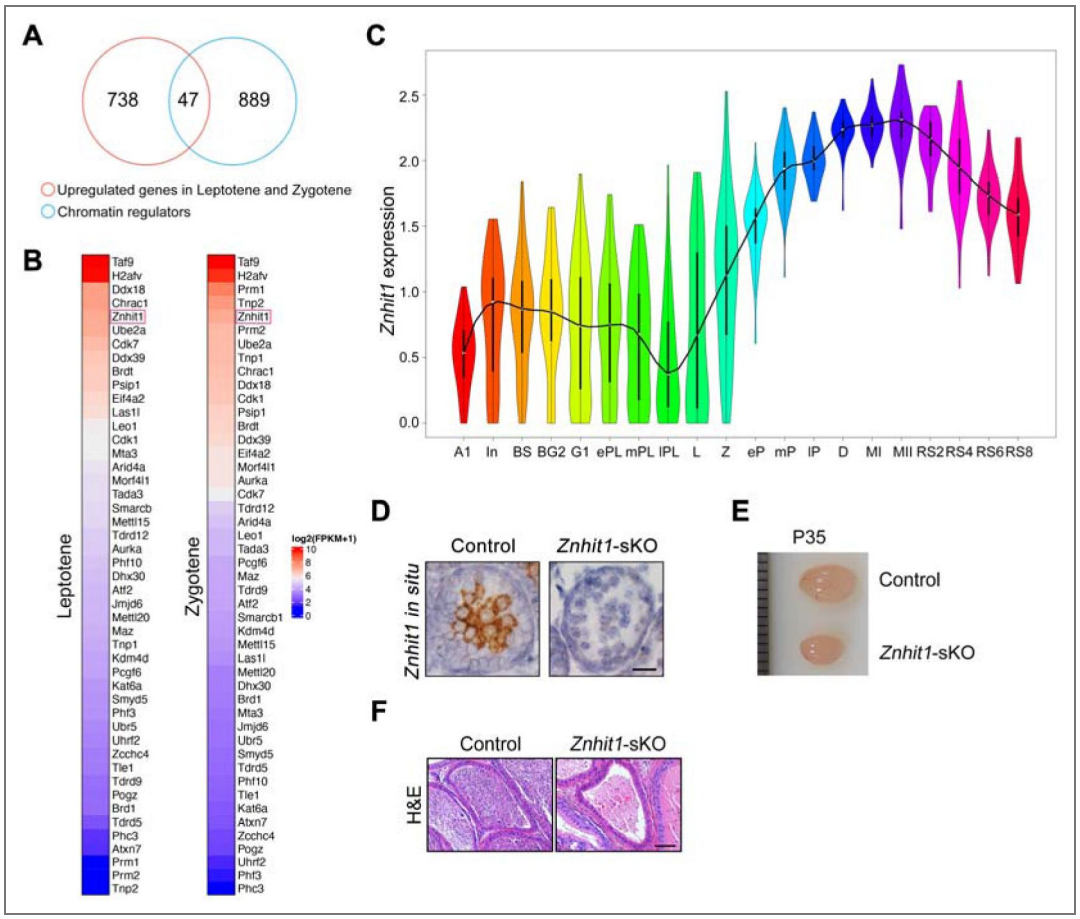

Figure S1. ***Znhit1*** **expression during meiotic progression and spermatocyte-conditional deletion of** ***Znhit1*** **with Stra8-cre.** (**A** and **B**) Venn diagram and heatmaps showing chromatin regulators highly expressed during leptotene and zygotene spermatocytes. (**C**) Violin plot showing *Znhit1* transcription level during spermatogenesis. Gene expression profiles derived from published scRNA-seq data (Chen et al, 2018). (**D**) *Znhit1* in situ hybridization in P14 testis sections. Scale bar, 20 μm. (**E**) Testis size comparison between control and *Znhit1*-sKO mice at P35. (**F**) Hematoxylin and eosin (H&E) - stained testis sections from control and *Znhit1*-sKO mice at P60. Scale bar, 50 μm.

Figure S2. Spermatocyte development in *Znhit1*-sKO testes.

(**A**) Immunostaining of SYCP3 and HSPA2 in testis sections of control or *Znhit1*-sKO mice at P35. Scale bar, 20 μm. (**B**) Immunostaining of SYCP3 and pH3 in testis sections of control or *Znhit1*-sKO mice at P35. Scale bar, 20 μm. (**C**) Immunostaining of H1T in testis sections from control and *Znhit1*-sKO mice at P35. Scale bar, 20 μm.

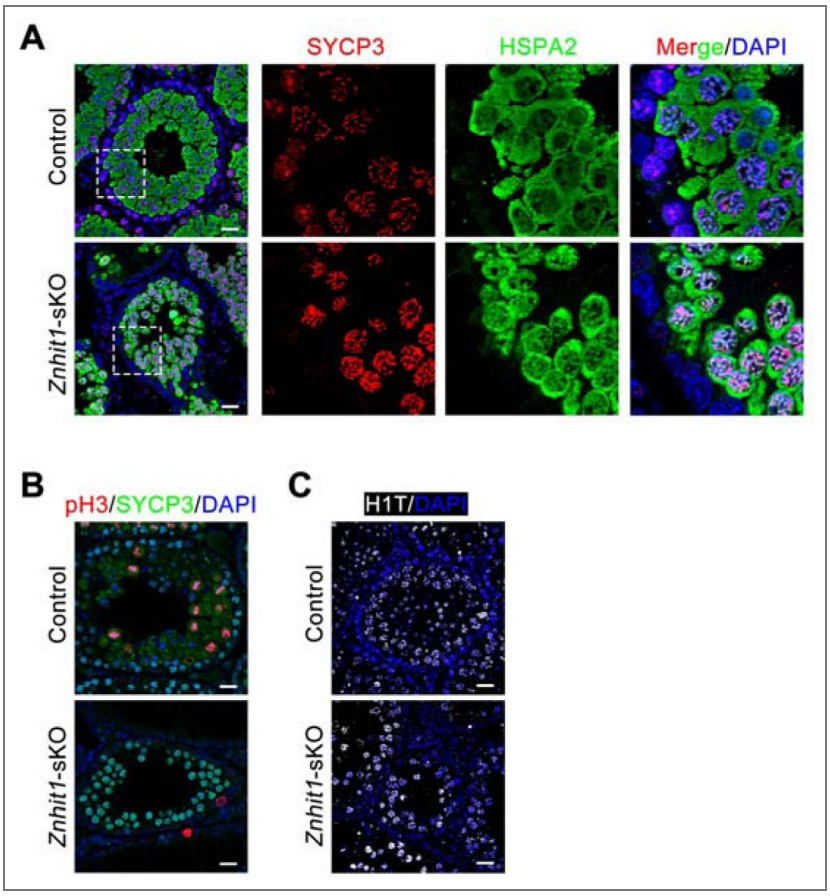

Figure S3. ZNHIT1 is required for meiotic recombination.

(**A** and **B**) Immunostaining of SYCP3 and RPA2 in spermatocyte chromosome spreads of control or *Znhit1*-sKO mice. Quantitative data are shown in (**B**). Scale bar, 10 μm. (**C**) Plots showing quantitative data of MLH1 foci of control or *Znhit1*-sKO mice. Data are presented as the mean ± s.d. *** $p < 0.001$

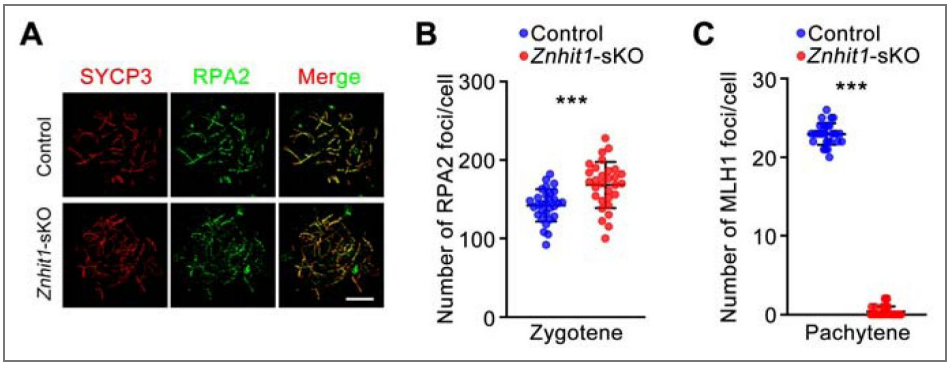

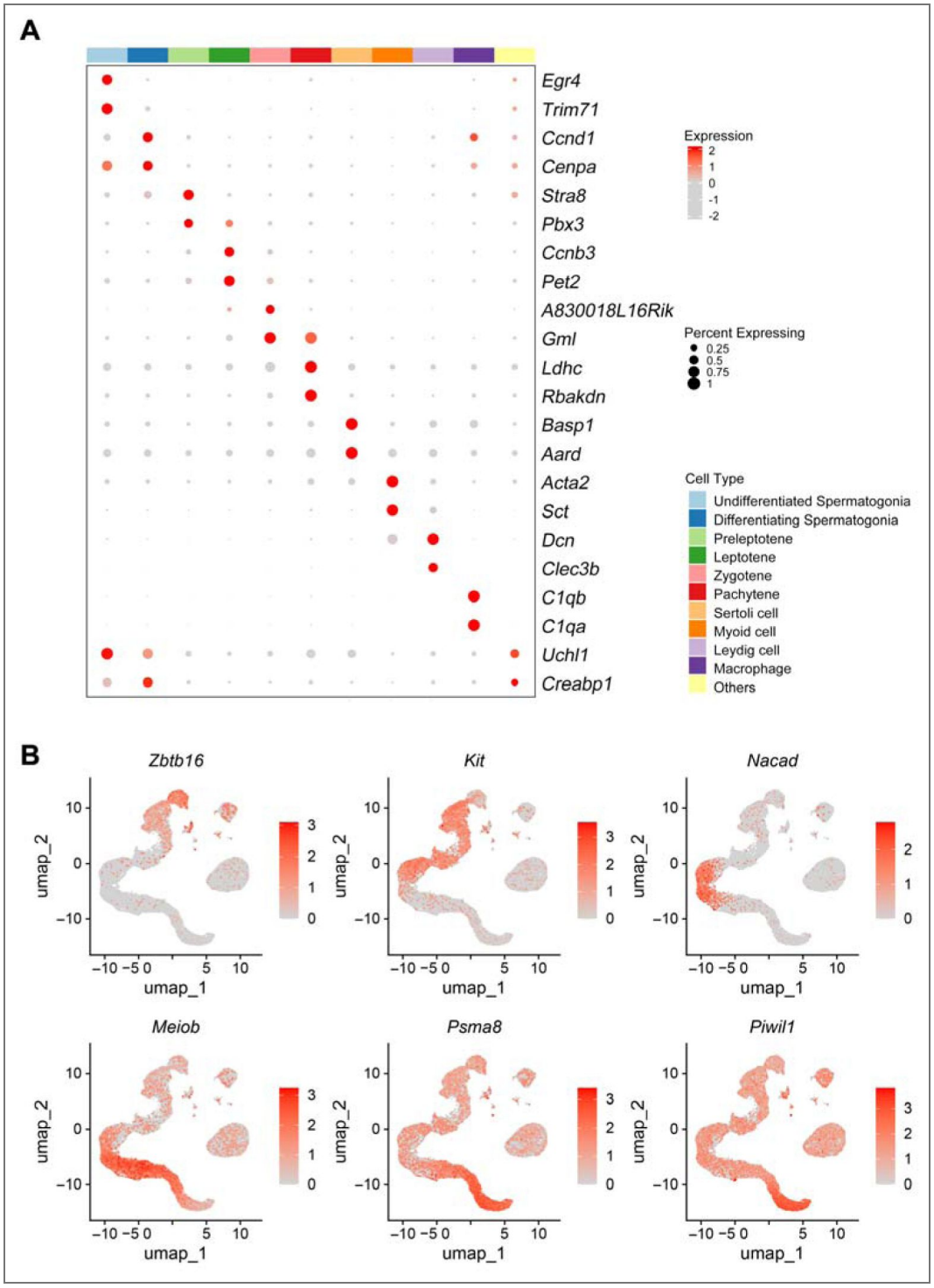

Figure S4. Single-cell RNA-seq of testicular cells.

(**A**) Dot plot showing the relative expression and the percentage of cells expressing selected markers across scRNA-seq clusters. (**B**) UMAP plots showing the normalized expression of the indicated genes in scRNA-seq data.

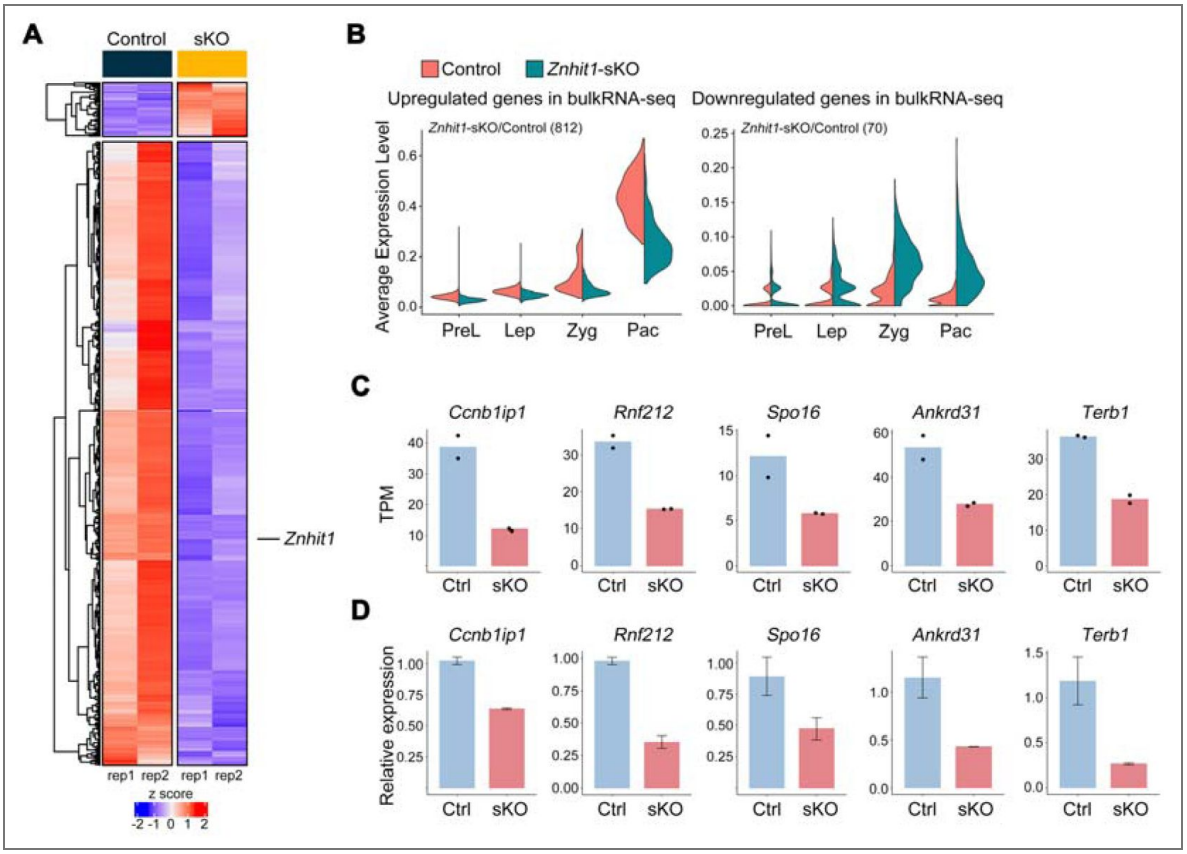

Figure S5. Transcriptomic analysis of testicular cells.

(**A**) Heatmap showing differentially expressed genes (DEGs) in P14 testicular cells between control and *Znhit1*-sKO mice. (**B**) Violin plots showing the average expression level of upregulated or downregulated genes between P14 control and *Znhit*1-sKO testicular cells. PreL, preleptotene; Lep, leptotene; Zyg, zygotene; Pac, pachytene. (**C** and **D**) Bar charts showing HR-related gene expression in P14 control and *Znhit*1-sKO testes. Data from bulk RNA-seq are shown in (**C**). Validated data from RT-qPCR are shown in (**D**). Ctrl, control; sKO, *Znhit1*-sKO.

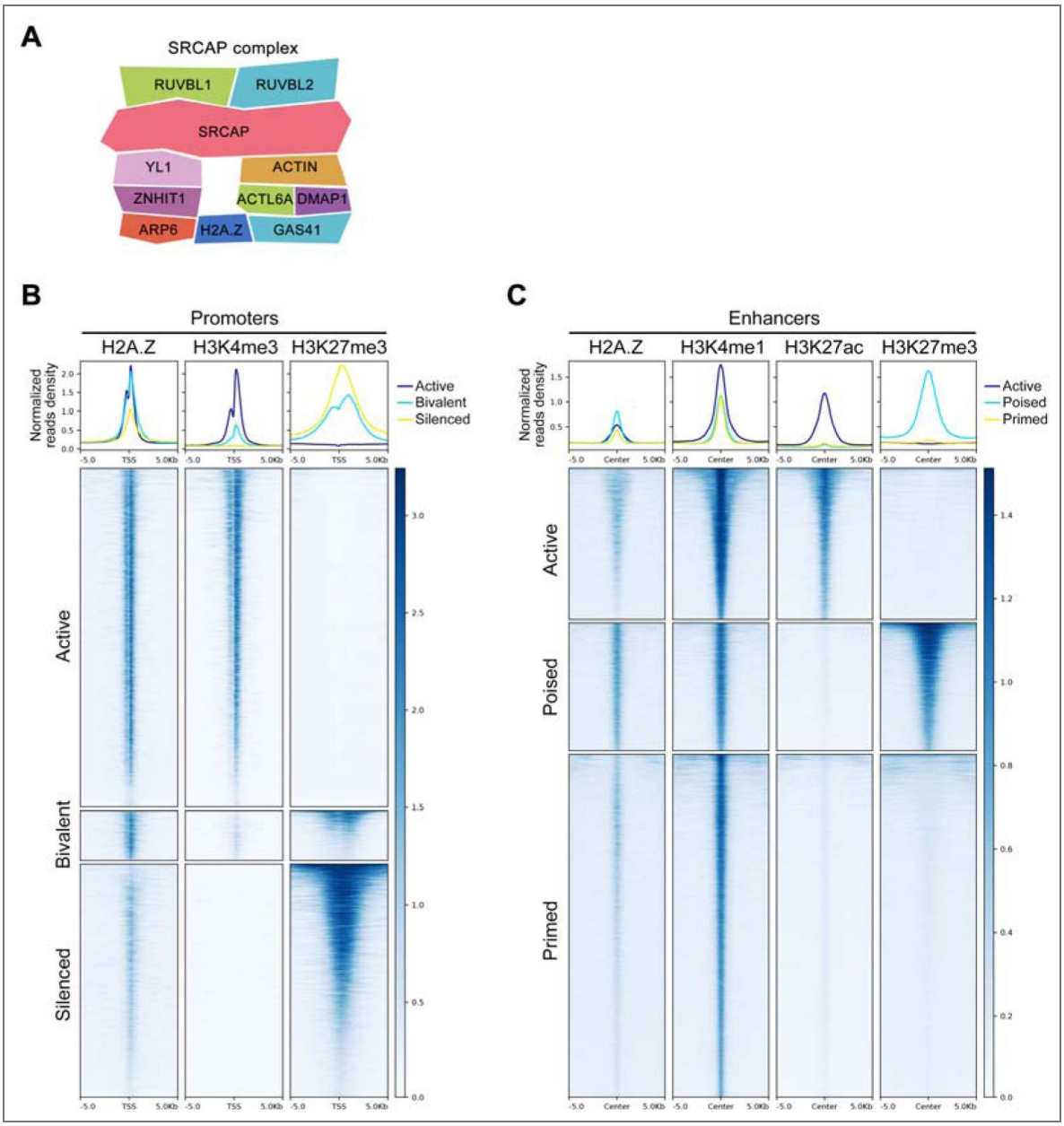

Figure S6. H2A.Z is enriched at meiotic gene promoters and enhancers.

(**A**) Schematic representation of the components of the SRCAP chromatin remodeling complex. (**B**) Heatmaps showing H2A.Z ChIP-seq signals surrounding different types of promoters. (**C**) Heatmaps showing H2A.Z ChIP-seq signals surrounding different types of enhancers.

Figure S7. *Znhit1* deletion downregulates the expression of A-MYB target genes.

(**A**) Violin plot showing the normalized expression of *Mybl1* in control and *Znhit1*-sKO spermatocytes at consecutive stages.
(**B**) Cluster annotation on the basis of the expression of A-MYB target genes in control or *Znhit1*-sKO testicular cells.

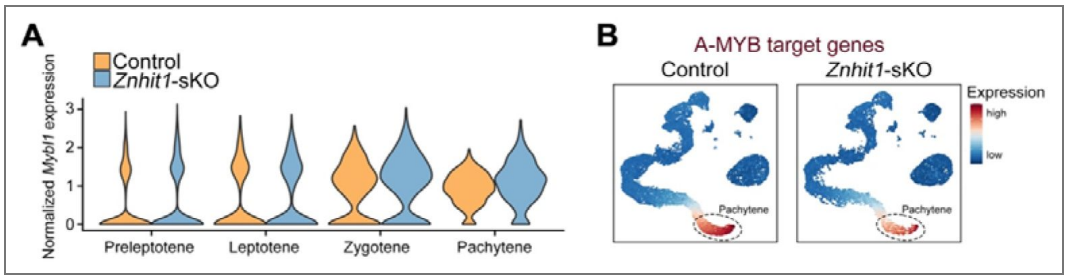

Figure S8. KAS-seq analysis.

(**A**) Mean plots of KAS-seq showing signal changes within indicated genes.

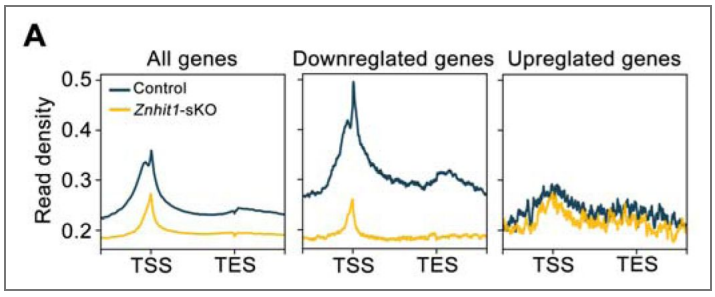

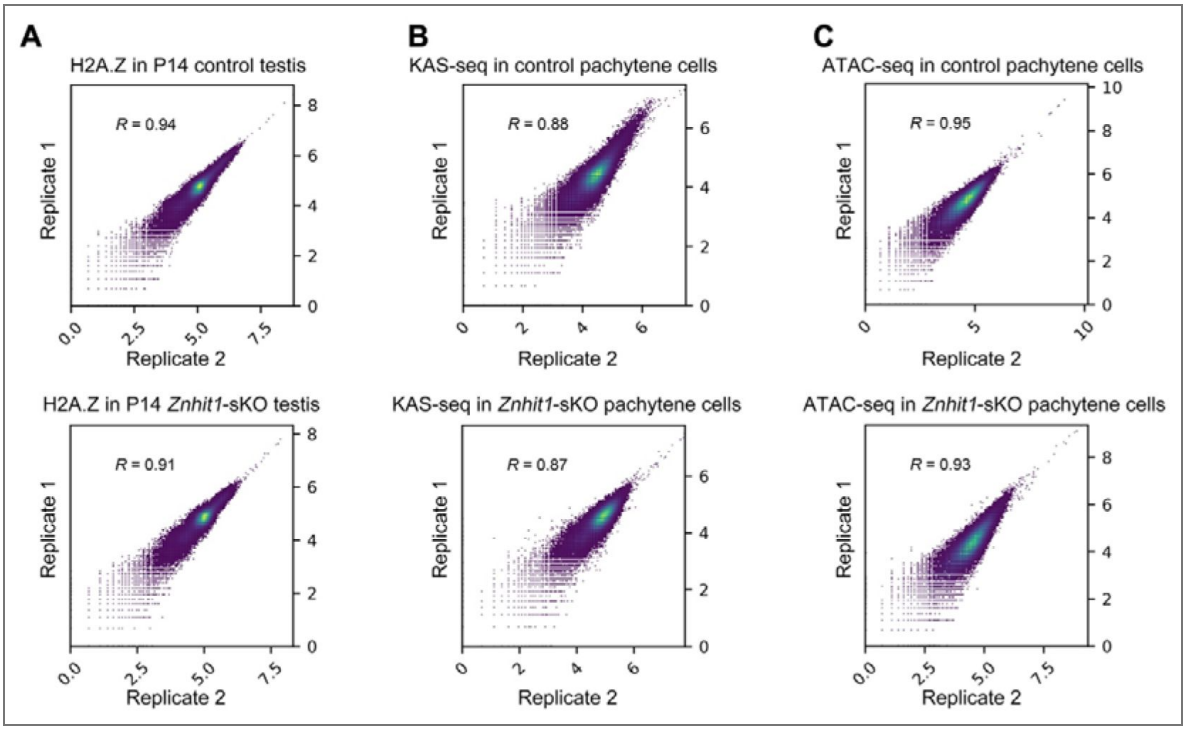

Figure S9. Reproducibility of replicates in this study.

(**A**) Scatter plots showing H2A.Z enrichments in P14 control or *Znhit1*-sKO testes for two independent H2A.Z ChIP-seq replicates. Pearson correlation coefficients are indicated. (**B**) Scatter plots showing KAS-seq signals in P14 control or *Znhit1*-sKO pachytene cells for two independent H2A.Z ChIP-seq replicates. Pearson correlation coefficients are indicated. (**C**) Scatter plots showing ATAC-seq signals in P14 control or *Znhit1*-sKO pachytene cells for two independent H2A.Z ChIP-seq replicates. Pearson correlation coefficients are indicated.

Data availability

The NGS data generated in this study were deposited in the NCBI SRA database under accession numbers SRP467214 (RNA-seq and ChIP-seq data) and SRP467448 (ATAC-seq and KAS-seq data).

Acknowledgements

We thank Chuan He for N3-kethoxal and Christopher L. Baker for meiotic chromatin state data.

Additional information

Funding

This work was supported by grants from the National Key Research and Development Program of China (2022YFA0806200, 2018YFC1003500, 2018YFA0800100, 2021YFC2501800), the National Natural Science Foundation of China (32192400, 81971443, 32300702, 32350710191), the Science and Technology Major Project of Inner Mongolia Autonomous Region of China to the State Key Laboratory of Reproductive Regulation and Breeding of Grassland Livestock (2020ZD0008). Shenfei Sun was supported by the fellowship of China Postdoctoral Science Foundation (2022M720797) and the Postdoctoral Fellowship Program (Grade B) of China Postdoctoral Science Foundation (GZB20230161).

Author Contributions

S.S. and X.L. conceived and designed the study; S.S. performed most of the experiments with the help of Y.J., Q.Z., H.P., F.H., X.Z., Y.G., X.Y., K.G., W.W., H.L., Z.S., Y.S., X.T., M.Y., and R.L.; Y.J. and N.J. performed the bioinformatics analysis; X.L. supervised the work and acquired the funding support; and S.S. and X.L. wrote the manuscript, with contributions from all authors.

Funding

Funder	Grant reference number	Author
MOST | National Key Research and Development Program of China (NKPs)	2022YFA0806200	Xinhua Lin
MOST | National Key Research and Development Program of China (NKPs)	2018YFC1003500	Xinhua Lin

Author ORCID iDs

Shenfei Sun: https://orcid.org/0000-0002-5034-4333

Additional files

Table S1. Chromatin factor genes targeted in gene expression analysis.

Table S2. Lists of changed genes between consecutive spermatocyte stages in scRNA-seq.

Table S3. GO analysis of PGA genes.

Table S4. Lists of DEGs between control and Znhit1-sKO in scRNA-seq.

Table S5. Lists of GO terms.

Table S6. List of DEGs in bulk RNA-seq.

Table S7. RT-qPCR primers used in this study.

Table S8. Markers of each cell type.

References

Adams S.R., Maezawa S., Alavattam K.G., Abe H., Sakashita A., Shroder M., Broering T.J., Sroga Rios J., Thomas M.A., Lin X., *et al.* (2018) RNF8 and SCML2 cooperate to regulate ubiquitination and H3K27 acetylation for escape gene activation on the sex chromosomes. *PLoS genetics* **14**:e1007233 https://doi.org/10.1371/journal.pgen.1007233 | PubMed

Aibar S., Gonzalez-Blas C.B., Moerman T., Huynh-Thu V.A., Imrichova H., Hulselmans G., Rambow F., Marine J.C., Geurts P., Aerts J., *et al.* (2017) SCENIC: single-cell regulatory network inference and clustering. *Nature methods* **14**:1083-1086 https://doi.org/10.1038/nmeth.4463 | PubMed

Alavattam K.G., Abe H., Sakashita A., Namekawa S.H (2018) Chromosome Spread Analyses of Meiotic Sex Chromosome Inactivation. *Methods in molecular biology (Clifton, NJ)* **1861**:113-129 https://doi.org/10.1007/978-1-4939-8766-5_10 | PubMed

Alexander A.K., Rice E.J., Lujic J., Simon L.E., Tanis S., Barshad G., Zhu L., Lama J., Cohen P.E., Danko C.G (2023) A-MYB and BRDT-dependent RNA Polymerase II pause release orchestrates transcriptional regulation in mammalian meiosis. *Nature communications* **14** https://doi.org/10.1038/s41467-023-37408-w | PubMed

Baudat F., Imai Y., de Massy B. (2013) Meiotic recombination in mammals: localization and regulation. *Nature reviews Genetics* **14**:794-806 https://doi.org/10.1038/nrg3573 | PubMed

Belotti E., Lacoste N., Simonet T., Papin C., Padmanabhan K., Scionti I., Gangloff Y.G., Ramos L., Dalkara D., Hamiche A., *et al.* (2020) H2A.Z is dispensable for both basal and activated transcription in post-mitotic mouse muscles. *Nucleic acids research* **48**:4601-4613 https://doi.org/10.1093/nar/gkaa157 | PubMed

Bergerat A., de Massy B., Gadelle D., Varoutas P.C., Nicolas A., Forterre P. (1997) An atypical topoisomerase II from Archaea with implications for meiotic recombination. *Nature* **386**:414-417 https://doi.org/10.1038/386414a0 | PubMed

Boekhout M., Karasu M.E., Wang J., Acquaviva L., Pratto F., Brick K., Eng D.Y., Xu J., Camerini-Otero R.D., Patel D.J., *et al.* (2019) REC114 Partner ANKRD31 Controls Number, Timing, and Location of Meiotic DNA Breaks. *Molecular cell* **74**:1053-1068 e1058 https://doi.org/10.1016/j.molcel.2019.03.023 | PubMed

Bolcun-Filas E., Bannister L.A., Barash A., Schimenti K.J., Hartford S.A., Eppig J.J., Handel M.A., Shen L., Schimenti J.C (2011) A-MYB (MYBL1) transcription factor is a master regulator of male meiosis. *Development* **138**:3319-3330 https://doi.org/10.1242/dev.067645 | PubMed

Butler A., Hoffman P., Smibert P., Papalexi E., Satija R (2018) Integrating single-cell transcriptomic data across different conditions, technologies, and species. *Nature biotechnology* **36**:411-420 https://doi.org/10.1038/nbt.4096 | PubMed

Cai Y., Jin J., Florens L., Swanson S.K., Kusch T., Li B., Workman J.L., Washburn M.P., Conaway R.C., Conaway J.W (2005) The mammalian YL1 protein is a shared subunit of the TRRAP/TIP60 histone acetyltransferase and SRCAP complexes. *The Journal of biological chemistry* **280**:13665-13670 https://doi.org/10.1074/jbc.m500001200 | PubMed

Cecchini K., Biasini A., Yu T., Saflund M., Mou H., Arif A., Eghbali A., Colpan C., Gainetdinov I., de Rooij D.G., *et al.* (2023) The transcription factor TCFL5 responds to A-MYB to elaborate the male meiotic program in mice. *Reproduction* **165**:183-196 https://doi.org/10.1530/rep-22-0355 | PubMed

Chen Y., Lyu R.T., Rong B.W., Zheng Y.X., Lin Z., Dai R.F., Zhang X., Xie N.N., Wang S.Q., Tang F.C., *et al.* (2020) Refined spatial temporal epigenomic profiling reveals intrinsic connection between PRDM9-mediated H3K4me3 and the fate of double-stranded breaks. *Cell research* **30**:256-268 https://doi.org/10.1038/s41422-020-0281-1 | PubMed

Chen Y., Zheng Y., Gao Y., Lin Z., Yang S., Wang T., Wang Q., Xie N., Hua R., Liu M., *et al.* (2018) Single-cell RNA-seq uncovers dynamic processes and critical regulators in mouse spermatogenesis. *Cell research* **28**:879-896 https://doi.org/10.1038/s41422-018-0074-y | PubMed

Choi K., Zhao X., Kelly K.A., Venn O., Higgins J.D., Yelina N.E., Hardcastle T.J., Ziolkowski P.A., Copenhaver G.P., Franklin F.C., *et al.* (2013) Arabidopsis meiotic crossover hot spots overlap with H2A.Z nucleosomes at gene promoters. *Nature genetics* **45**:1327-1336 https://doi.org/10.1038/ng.2766 | PubMed

Colino-Sanguino Y., Clark S.J., Valdes-Mora F (2022) The H2A.Z-nuclesome code in mammals: emerging functions. *Trends in genetics : TIG* **38**:273-289 https://doi.org/10.1016/j.tig.2021.10.003 | PubMed

Cuadrado A., Corrado N., Perdiguero E., Lafarga V., Munoz-Canoves P., Nebreda A.R (2010) Essential role of p18Hamlet/SRCAP-mediated histone H2A.Z chromatin incorporation in muscle differentiation. *The EMBO journal* **29**:2014-2025 https://doi.org/10.1038/emboj.2010.85 | PubMed

Cuadrado A., Lafarga V., Cheung P.C., Dolado I., Llanos S., Cohen P., Nebreda A.R. (2007) A new p38 MAP kinase-regulated transcriptional coactivator that stimulates p53-dependent apoptosis. *The EMBO journal* **26**:2115-2126 https://doi.org/10.1038/sj.emboj.7601657 | PubMed

Dong S., Han J., Chen H., Liu T., Huen M.S., Yang Y., Guo C., Huang J (2014) The Human SRCAP Chromatin Remodeling Complex Promotes DNA-End Resection. *Current biology : CB* **24**:2097-2110 https://doi.org/10.1016/j.cub.2014.07.081 | PubMed

Ernst C., Eling N., Martinez-Jimenez C.P., Marioni J.C., Odom D.T (2019) Staged developmental mapping and X chromosome transcriptional dynamics during mouse spermatogenesis. *Nature communications* **10**:1251 https://doi.org/10.1038/s41467-019-09182-1 | PubMed

Ernst J., Kellis M (2012) ChromHMM: automating chromatin-state discovery and characterization. *Nature methods* **9**:215-216 https://doi.org/10.1038/nmeth.1906 | PubMed

Feng Y., Zhang Y., Lin Z., Ye X., Lin X., Lv L., Lin Y., Sun S., Qi Y., Lin X (2022) Chromatin remodeler Dmp18 regulates apoptosis by controlling H2Av incorporation in Drosophila imaginal disc development. *PLoS genetics* **18**:e1010395 https://doi.org/10.1371/journal.pgen.1010395 | PubMed

Gaucher J., Boussouar F., Montellier E., Curtet S., Buchou T., Bertrand S., Hery P., Jounier S., Depaux A., Vitte A.L., *et al.* (2012) Bromodomain-dependent stage-specific male genome programming by Brdt. *The EMBO journal* **31**:3809-3820 https://doi.org/10.1038/emboj.2012.233 | PubMed

Gray S., Cohen P.E (2016) Control of Meiotic Crossovers: From Double-Strand Break Formation to Designation. *Annu Rev Genet* **50**:175-210 https://doi.org/10.1146/annurev-genet-120215-035111 | PubMed

Green C.D., Ma Q., Manske G.L., Shami A.N., Zheng X., Marini S., Moritz L., Sultan C., Gurczynski S.J., Moore B.B., *et al.* (2018) A Comprehensive Roadmap of Murine Spermatogenesis Defined by Single-Cell RNA-Seq. *Developmental cell* **46**:651-667 e610 https://doi.org/10.1016/j.devcel.2018.07.025 | PubMed

Gu Z., Hubschmann D. (2023) rGREAT: an R/bioconductor package for functional enrichment on genomic regions. *Bioinformatics* **39** https://doi.org/10.1093/bioinformatics/btac745 | PubMed

Handel M.A., Schimenti J.C (2010) Genetics of mammalian meiosis: regulation, dynamics and impact on fertility. *Nature reviews Genetics* **11**:124-136 https://doi.org/10.1038/nrg2723 | PubMed

Hassold T., Hunt P (2001) To err (meiotically) is human: the genesis of human aneuploidy. *Nature reviews Genetics* **2**:280-291 https://doi.org/10.1038/35066065 | PubMed

Heinz S., Benner C., Spann N., Bertolino E., Lin Y.C., Laslo P., Cheng J.X., Murre C., Singh H., Glass C.K (2010) Simple combinations of lineage-determining transcription factors prime cis-regulatory elements required for macrophage and B cell identities. *Molecular cell* **38**:576-589 https://doi.org/10.1016/j.molcel.2010.05.004 | PubMed

Hirota T., Blakeley P., Sangrithi M.N., Mahadevaiah S.K., Encheva V., Snijders A.P., Ellnati E., Ojarikre O.A., de Rooij D.G., Niakan K.K., *et al.* (2018) SETDB1 Links the Meiotic DNA Damage Response to Sex Chromosome Silencing in Mice. *Developmental cell* **47**:645 https://doi.org/10.1016/j.devcel.2018.10.004 | PubMed

Huang Y., Roig I (2023) Genetic control of meiosis surveillance mechanisms in mammals. *Front Cell Dev Biol* **11**:1127440 https://doi.org/10.3389/fcell.2023.1127440 | PubMed

Hunter N (2015) Meiotic Recombination: The Essence of Heredity. *Cold Spring Harbor perspectives in biology* **7** https://doi.org/10.1101/cshperspect.a016618 | PubMed

Kechin A., Boyarskikh U., Kel A., Filipenko M (2017) cutPrimers: A New Tool for Accurate Cutting of Primers from Reads of Targeted Next Generation Sequencing. *J Comput Biol* **24**:1138-1143 https://doi.org/10.1089/cmb.2017.0096 | PubMed

Keeney S., Giroux C.N., Kleckner N (1997) Meiosis-specific DNA double-strand breaks are catalyzed by Spo11, a member of a widely conserved protein family. *Cell* **88**:375-384 https://doi.org/10.1016/s0092-8674(00)81876-0 | PubMed

Kim D., Langmead B., Salzberg S.L (2015) HISAT: a fast spliced aligner with low memory requirements. *Nature methods* **12**:357-360 https://doi.org/10.1038/nmeth.3317 | PubMed

Kim D., Paggi J.M., Park C., Bennett C., Salzberg S.L (2019) Graph-based genome alignment and genotyping with HISAT2 and HISAT-genotype. *Nature biotechnology* **37**:907-915 https://doi.org/10.1038/s41587-019-0201-4 | PubMed

Kota S.K., Feil R (2010) Epigenetic transitions in germ cell development and meiosis. *Developmental cell* **19**:675-686 https://doi.org/10.1016/j.devcel.2010.10.009 | PubMed

Langmead B., Trapnell C., Pop M., Salzberg S.L (2009) Ultrafast and memory-efficient alignment of short DNA sequences to the human genome. *Genome biology* **10**:R25 https://doi.org/10.1186/gb-2009-10-3-r25 | PubMed

Lascarez-Lagunas L., Martinez-Garcia M., Colaiacovo M (2020) SnapShot: Meiosis - Prophase I. *Cell* **181**:1442-1442 e1441 https://doi.org/10.1016/j.cell.2020.04.038 | PubMed

Latendresse J.R., Warbrittion A.R., Jonassen H., Creasy D.M (2002) Fixation of testes and eyes using a modified Davidson's fluid: comparison with Bouin's fluid and conventional Davidson's fluid. *Toxicol Pathol* **30**:524-533 https://doi.org/10.1080/01926230290105721 | PubMed

Law N.C., Oatley M.J., Oatley J.M (2019) Developmental kinetics and transcriptome dynamics of stem cell specification in the spermatogenic lineage. *Nature communications* **10**:2787 https://doi.org/10.1038/s41467-019-10596-0 | PubMed

Li H., Durbin R (2009) Fast and accurate short read alignment with Burrows-Wheeler transform. *Bioinformatics* **25**:1754-1760 https://doi.org/10.1093/bioinformatics/btp324 | PubMed

Li H., Handsaker B., Wysoker A., Fennell T., Ruan J., Homer N., Marth G., Abecasis G., Durbin R., Genome Project Data Processing, S (2009) The Sequence Alignment/Map format and SAMtools. *Bioinformatics* **25**:2078-2079 https://doi.org/10.1093/bioinformatics/btp352 | PubMed

Li X.Z., Roy C.K., Dong X., Bolcun-Filas E., Wang J., Han B.W., Xu J., Moore M.J., Schimenti J.C., Weng Z., *et al.* (2013) An ancient transcription factor initiates the burst of piRNA production during early meiosis in mouse testes. *Molecular cell* **50**:67-81 https://doi.org/10.1016/j.molcel.2013.02.016 | PubMed

Lin Z., Hsu P.J., Xing X., Fang J., Lu Z., Zou Q., Zhang K.J., Zhang X., Zhou Y., Zhang T., *et al.* (2017) Mettl3-/Mettl14-mediated mRNA N6-methyladenosine modulates murine spermatogenesis. *Cell research* https://doi.org/10.1038/cr.2017.117 | PubMed

Long J., Huang C., Chen Y., Zhang Y., Shi S., Wu L., Liu Y., Liu C., Wu J., Lei M (2017) Telomeric TERB1-TRF1 interaction is crucial for male meiosis. *Nat Struct Mol Biol* **24**:1073-1080 https://doi.org/10.1038/nsmb.3496 | PubMed

Love M.I., Huber W., Anders S (2014) Moderated estimation of fold change and dispersion for RNA-seq data with DESeq2. *Genome biology* **15**:550 https://doi.org/10.1186/s13059-014-0550-8 | PubMed

Lu J., An J., Wang J., Cao X., Cao Y., Huang C., Jiao S., Yan D., Lin X., Zhou X (2022) Znhit1 Regulates p21Cip1 to Control Mouse Lens Differentiation. *Investigative ophthalmology & visual science* **63**:18 https://doi.org/10.1167/iovs.63.4.18 | PubMed

Maezawa S., Sakashita A., Yukawa M., Chen X., Takahashi K., Alavattam K.G., Nakata I., Weirauch M.T., Barski A., Namekawa S.H (2020) Super-enhancer switching drives a burst in gene expression at the mitosis-to-meiosis transition. *Nat Struct Mol Biol* **27**:978-988 https://doi.org/10.1038/s41594-020-0488-3 | PubMed

Manterola M., Brown T.M., Oh M.Y., Garyn C., Gonzalez B.J., Wolgemuth D.J. (2018) BRDT is an essential epigenetic regulator for proper chromatin organization, silencing of sex chromosomes and crossover formation in male meiosis. *PLoS genetics* **14**:e1007209 https://doi.org/10.1371/journal.pgen.1007209 | PubMed

Marcet-Ortega M., Pacheco S., Martinez-Marchal A., Castillo H., Flores E., Jasin M., Keeney S., Roig I (2017) p53 and TAp63 participate in the recombination-dependent pachytene arrest in mouse spermatocytes. *PLoS genetics* **13**:e1006845 https://doi.org/10.1371/journal.pgen.1006845 | PubMed

Mytlis A., Kumar V., Qiu T., Deis R., Hart N., Levy K., Masek M., Shawahny A., Ahmad A., Eitan H., *et al.* (2022) Control of meiotic chromosomal bouquet and germ cell morphogenesis by the zygotene cilium. *Science* eabh3104 https://doi.org/10.1126/science.abh3104 | PubMed

Ozata D.M., Yu T., Mou H., Gainetdinov I., Colpan C., Cecchini K., Kaymaz Y., Wu P.H., Fan K., Kucukural A., *et al.* (2020) Evolutionarily conserved pachytene piRNA loci are highly divergent among modern humans. *Nat Ecol Evol* **4**:156-168 https://doi.org/10.1038/s41559-019-1065-1 | PubMed

Papanikos F., Clement J.A.J., Testa E., Ravindranathan R., Grey C., Dereli I., Bondarieva A., Valerio-Cabrera S., Stanzione M., Schleiffer A., *et al.* (2019) Mouse ANKRD31 Regulates Spatiotemporal Patterning of Meiotic Recombination Initiation and Ensures Recombination between X and Y Sex Chromosomes. *Molecular cell* **74**:1069-1085 e1011 https://doi.org/10.1016/j.molcel.2019.03.022 | PubMed

Pertea M., Kim D., Pertea G.M., Leek J.T., Salzberg S.L (2016) Transcript-level expression analysis of RNA-seq experiments with HISAT, StringTie and Ballgown. *Nature protocols* **11**:1650-1667 https://doi.org/10.1038/nprot.2016.095 | PubMed

Pertea M., Pertea G.M., Antonescu C.M., Chang T.C., Mendell J.T., Salzberg S.L (2015) StringTie enables improved reconstruction of a transcriptome from RNA-seq reads. *Nature biotechnology* **33**:290-295 https://doi.org/10.1038/nbt.3122 | PubMed

Qiao H., Prasada Rao H.B., Yang Y., Fong J.H., Cloutier J.M., Deacon D.C., Nagel K.E., Swartz R.K., Strong E., Holloway J.K., *et al.* (2014) Antagonistic roles of ubiquitin ligase HEI10 and SUMO ligase RNF212 regulate meiotic recombination. *Nature genetics* **46**:194-199 https://doi.org/10.1038/ng.2858 | PubMed

Rabbani M., Zheng X., Manske G.L., Vargo A., Shami A.N., Li J.Z., Hammoud S.S (2022) Decoding the Spermatogenesis Program: New Insights from Transcriptomic Analyses. *Annu Rev Genet* **56**:339-368 https://doi.org/10.1146/annurev-genet-080320-040045 | PubMed

Ramirez F., Dundar F., Diehl S., Gruning B.A., Manke T (2014) deepTools: a flexible platform for exploring deep-sequencing data. *Nucleic acids research* **42**:W187-191 https://doi.org/10.1093/nar/gku365 | PubMed

Rao H.B., Qiao H., Bhatt S.K., Bailey L.R., Tran H.D., Bourne S.L., Qiu W., Deshpande A., Sharma A.N., Beebout C.J., *et al.* (2017) A SUMO-ubiquitin relay recruits proteasomes to chromosome axes to regulate meiotic recombination. *Science* **355**:403-407 https://doi.org/10.1126/science.aaf6407 | PubMed

Reynolds A., Qiao H.Y., Yang Y., Chen J.K., Jackson N., Biswas K., Holloway J.K., Baudat F., de Massy B., Wang J., *et al.* (2013) RNF212 is a dosage-sensitive regulator of crossing-over during mammalian meiosis. *Nature genetics* **45**:269-278 https://doi.org/10.1038/ng.2541 | PubMed

Roeder G.S., Bailis J.M (2000) The pachytene checkpoint. *Trends in genetics : TIG* **16**:395-403 https://doi.org/10.1016/s0168-9525(00)02080-1 | PubMed

Royo H., Prosser H., Ruzankina Y., Mahadevaiah S.K., Cloutier J.M., Baumann M., Fukuda T., Hoog C., Toth A., de Rooij D.G., *et al.* (2013) ATR acts stage specifically to regulate multiple aspects of mammalian meiotic silencing. *Genes & development* **27**:1484-1494 https://doi.org/10.1101/gad.219477.113 | PubMed

San Filippo J., Sung P., Klein H. (2008) Mechanism of eukaryotic homologous recombination. *Annual review of biochemistry* **77**:229-257 https://doi.org/10.1146/annurev.biochem.77.061306.125255 | PubMed

Shibuya H., Ishiguro K., Watanabe Y (2014) The TRF1-binding protein TERB1 promotes chromosome movement and telomere rigidity in meiosis. *Nature cell biology* **16**:145-156 https://doi.org/10.1038/ncb2896 | PubMed

Spruce C., Dlamini S., Ananda G., Bronkema N., Tian H., Paigen K., Carter G.W., Baker C.L (2020) HELLS and PRDM9 form a pioneer complex to open chromatin at meiotic recombination hot spots. *Genes & development* **34**:398-412 https://doi.org/10.1101/gad.333542.119 | PubMed

Subramanian A., Tamayo P., Mootha V.K., Mukherjee S., Ebert B.L., Gillette M.A., Paulovich A., Pomeroy S.L., Golub T.R., Lander E.S., *et al.* (2005) Gene set enrichment analysis: a knowledge-based approach for interpreting genome-wide expression profiles. *Proceedings of the National Academy of Sciences of the United States of America* **102**:15545-15550 https://doi.org/10.1073/pnas.0506580102 | PubMed

Subramanian V.V., Hochwagen A (2014) The meiotic checkpoint network: step-by-step through meiotic prophase. *Cold Spring Harbor perspectives in biology* **6**:a016675 https://doi.org/10.1101/cshperspect.a016675 | PubMed

Sun S., Jiang N., Jiang Y., He Q., He H., Wang X., Yang L., Li R., Liu F., Lin X., *et al.* (2020) Chromatin remodeler Znhit1 preserves hematopoietic stem cell quiescence by determining the accessibility of distal enhancers. *Leukemia* **34**:3348-3358 https://doi.org/10.1038/s41375-020-0988-5 | PubMed

Sun S., Jiang Y., Zhang Q., Pan H., Li X., Yang L., Huang M., Wei W., Wang X., Qiu M., *et al.* (2022) Znhit1 controls meiotic initiation in male germ cells by coordinating with Stra8 to activate meiotic gene expression. *Developmental cell* **57**:901-913 e904 https://doi.org/10.1016/j.devcel.2022.03.006 | PubMed

Symington L.S (2014) End resection at double-strand breaks: mechanism and regulation. *Cold Spring Harbor perspectives in biology* **6** https://doi.org/10.1101/cshperspect.a016436 | PubMed

Turner J.M (2015) Meiotic Silencing in Mammals. *Annu Rev Genet* **49**:395-412 https://doi.org/10.1146/annurev-genet-112414-055145 | PubMed

Turner J.M., Mahadevaiah S.K., Fernandez-Capetillo O., Nussenzweig A., Xu X., Deng C.X., Burgoyne P.S (2005) Silencing of unsynapsed meiotic chromosomes in the mouse. *Nature genetics* **37**:41-47 https://doi.org/10.1038/ng1484 | PubMed

Wang L., Xu Z., Khawar M.B., Liu C., Li W (2017) The histone codes for meiosis. *Reproduction* **154**:R65-R79 https://doi.org/10.1530/rep-17-0153 | PubMed

Wang Y., Chen Y., Chen J., Wang L., Nie L., Long J., Chang H., Wu J., Huang C., Lei M (2019) The meiotic TERB1-TERB2-MAJIN complex tethers telomeres to the nuclear envelope. *Nature communications* **10**:564 https://doi.org/10.1038/s41467-019-08437-1 | PubMed

Wang Y., Copenhaver G.P (2018) Meiotic Recombination: Mixing It Up in Plants. *Annu Rev Plant Biol* **69**:577-609 https://doi.org/10.1146/annurev-arplant-042817-040431 | PubMed

Wei W., Tang X., Jiang N., Ni C., He H., Sun S., Yu M., Yu C., Qiu M., Yan D., *et al.* (2022) Chromatin remodeler Znhit1 controls bone morphogenetic protein signaling in embryonic lung tissue branching. *The Journal of biological chemistry* **298**:102490 https://doi.org/10.1016/j.jbc.2022.102490 | PubMed

Wu T., Hu E., Xu S., Chen M., Guo P., Dai Z., Feng T., Zhou L., Tang W., Zhan L., *et al.* (2021) clusterProfiler 4.0: A universal enrichment tool for interpreting omics data. *Innovation (Camb)* **2**:100141 https://doi.org/10.1016/j.xinn.2021.100141 | PubMed

Xu M., Yao J., Shi Y., Yi H., Zhao W., Lin X., Yang Z (2021) The SRCAP chromatin remodeling complex promotes oxidative metabolism during prenatal heart development. *Development* **148** https://doi.org/10.1242/dev.199026 | PubMed

Xu Y., Ayrapetov M.K., Xu C., Gursoy-Yuzugullu O., Hu Y., Price B.D (2012) Histone H2A.Z controls a critical chromatin remodeling step required for DNA double-strand break repair. *Molecular cell* **48**:723-733 https://doi.org/10.1016/j.molcel.2012.09.026 | PubMed

Yamada S., Kugou K., Ding D.Q., Fujita Y., Hiraoka Y., Murakami H., Ohta K., Yamada T (2018) The histone variant H2A.Z promotes initiation of meiotic recombination in fission yeast. *Nucleic acids research* **46**:609-620 https://doi.org/10.1093/nar/gkx1110 | PubMed

Yoshida S., Sukeno M., Nakagawa T., Ohbo K., Nagamatsu G., Suda T., Nabeshima Y (2006) The first round of mouse spermatogenesis is a distinctive program that lacks the self-renewing spermatogonia stage. *Development* **133**:1495-1505 https://doi.org/10.1242/dev.02316 | PubMed

Yoshida S., Takakura A., Ohbo K., Abe K., Wakabayashi J., Yamamoto M., Suda T., Nabeshima Y (2004) Neurogenin3 delineates the earliest stages of spermatogenesis in the mouse testis. *Developmental biology* **269**:447-458 https://doi.org/10.1016/j.ydbio.2004.01.036 | PubMed

Yu J., Sui F., Gu F., Li W., Yu Z., Wang Q., He S., Wang L., Xu Y (2024) Structural insights into histone exchange by human SRCAP complex. *Cell Discov* **10**:15 https://doi.org/10.1038/s41421-023-00640-1 | PubMed

Yu T., Fan K., Ozata D.M., Zhang G., Fu Y., Theurkauf W.E., Zamore P.D., Weng Z (2021) Long first exons and epigenetic marks distinguish conserved pachytene piRNA clusters from other mammalian genes. *Nature communications* **12**:73 https://doi.org/10.1038/s41467-020-20345-3 | PubMed

Zhang Q., Ji S.Y., Busayavalasa K., Yu C (2019) SPO16 binds SHOC1 to promote homologous recombination and crossing-over in meiotic prophase I. *Sci Adv* **5**:eaau9780 https://doi.org/10.1126/sciadv.aau9780 | PubMed

Zhang Y., Liu T., Meyer C.A., Eeckhoute J., Johnson D.S., Bernstein B.E., Nusbaum C., Myers R.M., Brown M., Li W., *et al.* (2008) Model-based analysis of ChIP-Seq (MACS). *Genome biology* **9**:R137 https://doi.org/10.1186/gb-2008-9-9-r137 | PubMed

Zhao B., Chen Y., Jiang N., Yang L., Sun S., Zhang Y., Wen Z., Ray L., Liu H., Hou G., *et al.* (2019) Znhit1 controls intestinal stem cell maintenance by regulating H2A.Z incorporation. *Nature communications* **10**:1071 https://doi.org/10.1038/s41467-019-09060-w | PubMed

Zheng H., Xie W (2019) The role of 3D genome organization in development and cell differentiation. *Nature reviews Molecular cell biology* https://doi.org/10.1038/s41580-019-0132-4 | PubMed

Zickler D., Kleckner N (2023) Meiosis: Dances Between Homologs. *Annu Rev Genet* https://doi.org/10.1146/annurev-genet-061323-044915 | PubMed

Sun et al (2024) NGS data in NCBI SRA database. SRP467214. ID PRJNA1029730 https://www.ebi.ac.uk/ena/browser/view/PRJNA1029730

Sun et al (2024) NGS data in NCBI SRA database. SRP467448. ID PRJNA1030084 https://www.ebi.ac.uk/ena/browser/view/PRJNA1030084

Chen et al (2018) scRNA-seq data of male germ cells. NCBI Gene Expression Omnibus. ID GSE107644 https://www.ncbi.nlm.nih.gov/geo/query/acc.cgi?acc=GSE107644

Li et al (2013) omics data of mouse testes. NCBI Gene Expression Omnibus. ID GSE44690 https://www.ncbi.nlm.nih.gov/geo/query/acc.cgi?acc=GSE44690

Peer reviews

Reviewer #1 (Public review):

Summary:

Sun et al. generated germline-specific cKO mice for the Znhit1 gene and examined its effect on male meiosis. The authors found that the loss of Znhit1 affects the transcriptional activation of pachytene. Znhit1 is a subunit of the SRCAP chromatin remodeling complex and a depositor of H2AZ, and in cKO spermatocytes, H2AZ is not deposited into the gene region.

The authors claim that this is why the PGA was not activated. These findings provide important insights into the mechanisms of transcriptional regulation during the meiotic prophase.

Strengths:

The authors used samples from their original mouse model, analyzing both the epigenome and the transcriptome in detail using diverse NGS analyses to gain new insights into PGA. The quality of the results appeared excellent.

Comments on revisions:

Sun et al. have responded to each comment with great care and sincerity, and substantial improvements are evident.

In particular, the addition of scRNA-seq data from P35 samples appears to play an important role in supporting the authors' claims.

However, there is still room for improvement in the reanalysis of the data and in the Discussion section.

From the data perspective, for example, the authors state in line 347 of the revised manuscript that "We found that Znhit1-deficient spermatocytes phenocopied abnormal meiotic phenotypes observed in A-MYB mutants." However, the corresponding descriptions in the main text and figure legends are not sufficiently detailed, and therefore do not fully support or substantiate this interpretation. Incorporating a statistical comparison between DEGs in Znhit1-sKO and A-myb KO would likely strengthen this point.

Regarding the overall structure of the Discussion, the connections among delayed DSB repair, MSCI, and PGA regulation via H2A.Z remain somewhat descriptive and difficult to follow. This may reflect a lack of direct evidence linking these processes; however, a more logically structured and clearly articulated Discussion would improve clarity.

https://doi.org/10.7554/eLife.99713.2.sa2

Reviewer #2 (Public review):

Summary:

The study demonstrates that Znhit1 regulates male meiosis, with deletion causing pachytene failure associated with defective expression of pachytene genes and subtle effects on X-Y pairing and DSB repair. The authors attribute this phenotype to the defective incorporation of the Znhit1 target H2A.Z into chromatin.

Strengths:

The paper and the figures are well presented and the narrative is clear. Evidence that the conditional deletion strategy removes Znhit1 is strong, with multiple orthogonal approaches used. Most of the meiotic phenotyping is well performed, and the omics analysis clearly identifies a dramatic effect on the meiotic gene expression program. The link to H2A.Z and A-MYB adds a mechanistic angle to the study.

Comments on revisions:

In the revision, the authors have addressed most of my comments. The only incomplete one is comment 1, where I asked them to define the stage of germ cell arrest by histology. I requested this because the stage of arrest they identified is so unique. They didn't do it, and

instead used the scRNAseq to show a depletion at the late pachytene stage onwards. I guess it supports their main findings, but it's a bit disappointing.

https://doi.org/10.7554/eLife.99713.2.sa1

Author response:

The following is the authors' response to the original reviews.

> ***Reviewer #1 (Public Review):***
>
> *Summary:*
>
> *Sun et al. generated germline-specific cKO mice for the Znhit1 gene and examined its effect on male meiosis. The authors found that the loss of Znhit1 affects the transcriptional activation of pachytene. Znhit1 is a subunit of the SRCAP chromatin remodeling complex and a depositor of H2AZ, and in cKO spermatocytes, H2AZ is not deposited into the gene region. The authors claim that this is why the PGA was not activated. These findings provide important insights into the mechanisms of transcriptional regulation during the meiotic prophase.*
>
> *Strengths:*
>
> *The authors used samples from their original mouse model, analyzing both the epigenome and the transcriptome in detail using diverse NGS analyses to gain new insights into PGA. The quality of the results appeared excellent.*
>
> *Weaknesses:*
>
> *Overall, the data is inconsistent with the authors' claims and does not support their final conclusions. In addition, the sample used may not be the most suitable for the analysis, but a more suitable sample would dramatically improve the overall quality of the paper.*

Thank you for your comprehensive summary of our study and your thoughtful insights into its strengths and weaknesses. We greatly appreciate this valuable feedback, which helps us further improve our work. Below, we provide a detailed response addressing each of the points you raised.

> ***Reviewer #1 (Recommendations For The Authors):***
>
> *Major revisions:*
>
> *Surprisingly, many genes were upregulated in the scRNA-seq results. How many XY genes are included? Discuss why many genes are up-regulated in Fig. 5E whereas bulk RNA-seq showed only 70 genes were down-regulated. Since apoptosis-related factors are up-regulated in Fig5E, could these up-regulated genes be due to the high content of the transcriptome of dead cells? As you know, cell death starts, but randomly and violently disrupts the transcriptome, so we think it is not desirable to analyze the transcriptome with dead cells in the mix. Describe this point appropriately in the text or generate new data without dead cells.*

We sincerely appreciate the reviewer's critical points. Below, we address each point sequentially:

(1) To address the question about XY-linked genes, we utilized scRNA-seq data to identify differentially expressed sex chromosome genes in spermatocytes at different stages. Our analysis revealed an aberrant activation of XY-linked genes relative to controls. Specifically, 120 XY-linked genes were aberrantly activated in zygotenestage spermatocytes, and 119 XY-

linked genes showed aberrant activation in pachytene-stage spermatocytes (revised Fig. 4F). This observation directly indicates that *Znhit1* knockout impairs Meiotic Sex Chromosome Inactivation (MSCI), a finding that aligns with our prior characterization of XY chromosome synapsis defects in *Znhit1*-deficient spermatocytes.

(2) Two key reasons explain the discrepancy between scRNA-seq and bulk RNA-seq results:

First, scRNA-seq employs a more permissive threshold for identifying DEGs (log2 fold change [log2FC] = 0.25), thereby enhancing sensitivity to subtle expression changes and enabling the detection of more upregulated genes. In contrast, bulk RNAseq uses a stricter threshold (log2FC = 1), which filters out these subtly upregulated transcripts, resulting in fewer DEGs overall.

Second, scRNA-seq can capture cell subset-specific differential expression. In contrast, bulk RNA-seq averages signals across mixed cells, masking such subsetspecific expression changes.

These clarifications have been included in the Data Analysis section of the revised manuscript.

(3) We fully agree with the reviewer's concern that dead cells could confound transcriptomic analyses. Before downstream analysis, we excluded non-viable cells via stringent QC: cells with mitochondrial RNA (mtRNA) content exceeding 15% were removed, as high mtRNA content is a well-established marker of cell death or compromised viability. To further validate that upregulated genes were not driven by dead cell contamination, we analyzed the correlation between the expression of apoptosis-related genes and mtRNA fractions in our data. This analysis revealed no significant correlation (Pearson correlation coefficient, r = -0.02; please see Author response image 1). These results collectively rule out dead cell transcriptome contamination as the primary cause of the observed gene upregulation.

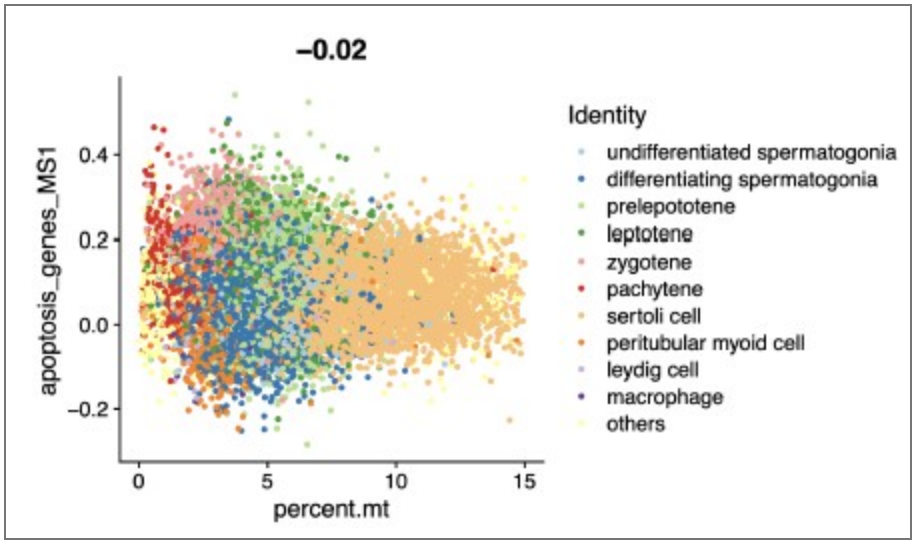

Author response image 1. Scatter Chart showing the Pearson correlation between apoptosisrelated genes and mitochondrial RNA fractions in scRNA-seq data.

> *Line 280-286: The data in Figures 7I and J are confusing: as shown by KAS-seq, it is natural that ssDNA is not formed in the promoter region in Znhit1-cKO sample because transcription does not proceed, but why is ssDNA formed in the enhancer region in the first place in control and then lost in Znhit1-cKO sample? Generally, it is said that in the enhancer region, including the super-enhancer region, doublestranded DNA is not dissociated, thus not forming ssDNA. Discuss why the loss of ssDNA in the enhancer*

> *region affects transcription with appropriate citations. Also, show whether genes downstream of the missing ssDNA in the promoter region have abnormal transcriptional activity, along with the RNA-seq data. Furthermore, in the region shown in Figure 7I, why the chromatin is even more open, as shown by ATACseq in Znhit1-cKO. Discuss whether this is related to transcriptional progression or aberrant substitution with H2A. If the function of ZNHIT1 is to replace H2A with H2AZ for PGA, it is not necessary to show the H2A level in Znhit1-cKO.*

We appreciate the reviewer's constructive comments.

(1) ssDNA dynamics in enhancer regions: Emerging evidence demonstrates that active enhancers undergo transient DNA unwinding to form ssDNA, a process critical for transcriptional regulation by transcribing enhancer RNAs (eRNA). KAS-seq is sufficiently sensitive to detect ssDNA in enhancer regions (Kim et al., 2010; Wu et al., 2020). It has been shown that H2A.Z (deposited by the ZNHIT1-SRCAP complex) is required for maintaining enhancer accessibility and dynamic unwinding (Sporrij et al., 2023). In this study, we found that *Znhit1* deletion and defective H2A.Z incorporation impaired enhancer ssDNA formation, indicating that ZNHIT-H2A.Z plays an important role in the activity of both promoter and enhancer.

(2) Impact of ssDNA loss on transcription: To address how missing ssDNA affects transcriptional activity, we further analyzed changes in KAS-seq signals following *Znhit1* knockout. Overall, KAS-seq signals were significantly reduced upon *Znhit1* depletion, confirming that *Znhit1* is essential for ssDNA formation. Further examination of KAS-seq signals at promoters of downregulated genes also revealed reduced signals (revised manuscript, Fig. S8). In contrast, KAS-seq signals of upregulated genes remained relatively low and showed no changes in both the control and knockout groups, and their upregulation probably results from indirect regulation. These results underscore the importance of ZNHIT1-mediated chromatin states in regulating ssDNA formation and gene expression.

(3) Aberrant chromatin openness in *Znhit1*-cKO (ATAC-seq): The increased chromatin accessibility detected by ATAC-seq likely represents a disorganized, nonfunctional state rather than productive transcriptional openness. H2A.Z normally constrains chromatin dynamics to facilitate ordered transcriptional regulation (Cole et al., 2021); its absence in *Znhit1*-cKO leads to higher ATAC-seq signals, suggesting that this aberrant openness fails to support proper assembly of the transcriptional machinery.

> *Minor revisions:*
>
> *Line 106. The text says that they looked for chromatin factors, but the legend says that they looked for epigenetic factors. The text must be consistent.*

We have corrected it in the revised manuscript (line 801).

> *Line 107. Although it is stated that the transcriptional data published here were used, it appears from the cited references that they are scRNA-seq data. A clear explanation is required in the text or legend.*

We have revised this data as scRNA-seq data (line 107).

> *Line 141-143: Using TUNEL analysis in Figure 4F, the authors show that Znhit1cKO testis cells contain many dead cells. Describe the type or stage of the apoptotic cells.*

We appreciate the reviewer's suggestion. Specifically, we performed TUNEL staining on testes isolated from P14 mice, a critical time point for pachytene development (revised Fig. 2D). We tested this by showing that apoptosis-related genes were significantly upregulated in pachytene-stage spermatocytes in scRNA-seq data (revised Fig. 4D). To further validate this

observation, we performed scRNA-seq from P35 testis samples. The results revealed a significant reduction in late pachytene-stage spermatocytes in *Znhit1*-cKO samples (revised Fig. 2F), consistent with apoptotic loss of pachytene cells. Collectively, these data confirm that *Znhit1* knockout impairs pachytene-stage spermatocyte development.

> *The authors claimed that the loss of Znhit1 lowers the transcription of a group of genes involved in homologous recombination, including Rnf212, causing a delay in homologous recombination; however, if the process of homologous recombination is delayed, homologous chromosome pairing and synapsis are affected unless DSB repair is completed. Provide a satisfactory explanation for the fact that DNA damage remains on autosomes despite complete synapsis, as shown in Figure 3C, which is likely not solely due to delayed homologous recombination.*

Thank you for this insightful comment. We fully agree that persistent autosomal DNA damage cannot be explained solely by delayed homologous recombination. To resolve this question, we further analyzed autosomal synapsis through SYCP1 and SYCP3 staining. While autosomal synapsis appeared morphologically complete, we identified subtle but significant synapsis defects in autosomal terminal regions (revised Fig. 3A). This suggests that *Znhit1* knockout also results in autosomal synapsis defects. We speculate that these synapsis defects are associated with the unresolved autosomal DNA damage we observed.

> *Lines 150-163. With regard to XY unpairing in Znhit1-cKO pachytene spermatocytes, there is insufficient discussion as to whether this is due to transcriptional aberrations.*

Thank you for highlighting the need to link transcriptional aberrations to XY unpairing in *Znhit1*-cKO pachytene spermatocytes. To address this, we analyzed sex chromosome transcription using scRNA-seq data. Relative to controls, 120 XYlinked genes were aberrantly activated at zygotene, and 119 were upregulated at pachytene in *Znhit1*-cKO spermatocytes (revised Fig. 4F), directly demonstrating *Znhit1* knockout disrupts Meiotic Sex Chromosome Inactivation (MSCI). Given that intact MSCI is required to stabilize XY synapsis in pachytene spermatocytes, we conclude that the observed XY unpairing is likely a direct consequence of these sex chromosome transcriptional abnormalities. We add this information to the revised manuscript (lines 221-226).

> *Line 187-194. Analysis of the scRNA-seq data is shown in Figure 4, but it lists several genes as stage-specific markers, some of which do not have well-understood meiotic functions. Please cite a reference paper that provides sufficient evidence to qualify this stage.*

In response to this comment, we have refined the presentation of marker genes used for cell annotation (revised Fig. S4B). We have incorporated relevant references supporting their utility as stage-specific markers for the meiotic stages (line 187).

> *Line 225-233: If Znhit1 is important for H2AZ deposition and regulates PGA through it, how does it regulate HR-related genes that are expressed earlier through H2AZ deposition during the pachytene stage? For example, Rnf212 is not specifically expressed during the pachytene stage but is one of the targets of MEIOSIN, so it is expressed at an earlier stage.*

Thank you for this insightful comment. We fully acknowledge the reviewer's key observation that HR-related genes such as *Rnf212* are MEIOSIN targets that initiate transcription at earlier meiotic stages, before the pachytene stage. Our stage-resolved scRNA-seq data further showed that the expression of *Ccnb1ip1* and *Rnf212* was significantly upregulated from zygotene to pachytene, following their initial transcriptional onset. We next showed that the loss of H2A.Z deposition induced by *Znhit1* deletion specifically impaired this pachytene-specific secondary transcriptional activation, rather than the early MEIOSIN-driven expression onset (please see Author response image 2).

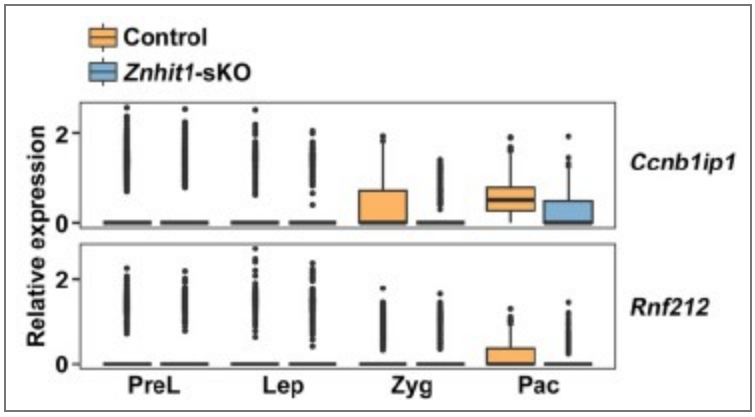

Author response image 2. **Plots showing the expression level of indicated genes in scRNAseq data.**

> *Line 245-251: As shown in Figure 6E, more than 14,000 genes have H2AZ peaks. In contrast, only approximately 60% of the genes downregulated by Znhit1-cKO appeared to be directly affected by H2AZ. Are the remaining 40% of genes regulated in a different way that is not mediated by H2AZ? Also, only a few percent of the genes with H2AZ peaks are affected, but why are only genes with A-MYB involvement affected, as shown in Figure 7?*

Thank you for these insightful and constructive comments. For the ~40% of downregulated genes not directly linked to H2A.Z, they were likely regulated through indirect mechanisms. H2A.Z deposition mediated by ZNHIT1 may influence upstream transcriptional regulators (e.g., transcription factors or coactivators), whose dysregulation in turn affects these genes.

The selective effect of H2A.Z loss on A-MYB target genes is explained by the strict context-dependent function of H2A.Z, which requires stage-specific partner transcription factors to exert its regulatory activity. During the zygotene-to-pachytene transition, A-MYB acts as the master regulator of pachytene gene activation and forms a functional collaborative complex with H2A.Z to drive target gene transcription. Disrupted H2A.Z deposition upon *Znhit1* deletion specifically impairs the activity of this A-MYB-H2A.Z complex, leading to selective downregulation of A-MYB targets. Other H2A.Z peak-associated genes may rely on alternative cofactors and compensatory mechanisms.

> *Line 245-256: Figures 6 and F show that the localization of H2AZ is reduced in Znhit1-cKO mice, which means that no substitution with H2A occurs. If so, show it in the data because the localization of H2A should be increased compared to that in the control.*

To clarify the status of H2A, we have now detected immunofluorescent staining against H2A. While H2A.Z deposition was clearly impaired following *Znhit1* deletion, the global level of H2A did not change significantly (Author response image 3). We speculate that this observed absence of a compensatory increase in H2A is likely due to the intrinsically low abundance of the histone variant H2A.Z relative to canonical histone H2A under physiological conditions.

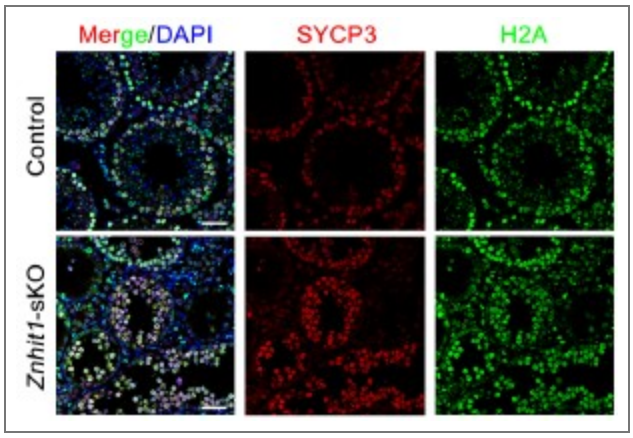

Author response image 3. **Immunostaining of SYCP3 and H2A in spermatocyte testis sections of control and *Znhit1*-sKO mice, Scale bar, 40 μm.**

> ***Reviewer #2 (Public Review):***
>
> *Summary:*
>
> *The study demonstrates that Znhit1 regulates male meiosis, with deletion causing pachytene failure associated with defective expression of pachytene genes and subtle effects on X-Y pairing and DSB repair. The authors attribute this phenotype to the defective incorporation of the Znhit1 target H2A.Z into chromatin.*
>
> *Strengths:*
>
> *The paper and the figures are well presented and the narrative is clear. Evidence that the conditional deletion strategy removes Znhit1 is strong, with multiple orthogonal approaches used. Most of the meiotic phenotyping is well performed, and the omics analysis clearly identifies a dramatic effect on the meiotic gene expression program. The link to H2A.Z and A-MYB adds a mechanistic angle to the study.*
>
> *Weaknesses:*
>
> *(1) Current literature demonstrates that meiotic mutants arrest at one of two stages: midpachytene (stage IV of the seminiferous cycle) or metaphase I (stage XII of the seminiferous cycle). This study documents that in the Znhit1 KO the midpachytene marker H1t appears normally, but that cells arrest before diplotene. If this is true, then arrest must occur during late pachytene, which based on my knowledge has never been documented for a meiotic KO. To resolve this, the authors should present stronger histological substaging evidence to support their claim.*

Thank you for this insightful and constructive comment. To achieve highresolution tracking of cell lineage progression, we performed scRNA-seq analysis using P35 testes in this revised manuscript. scRNA-seq data showed that germ cells normally progressed through all meiotic stages and successfully gave rise to spermatids in control groups. By contrast, in the *Znhit1* knockout group, late pachytene spermatocytes decreased significantly, and only very few subsequent germ cell types were observable (revised Fig. 2F, G). In scRNA-seq data, although very few diplotene spermatocytes and meiotic metaphase I cells were detectable, these cells still appeared abnormal, as evidenced by their extremely low *Pou5f2* expression. We have revised our description of the meiotic arrest stage in the manuscript.

> *(2) The authors overlooked the possible effects of Znhit1 deletion on MSCI. Defective MSCI is a well-established cause of pachytene arrest. Actually, the fact that they see X-Y pairing failure should alert them even more strongly to this possibility because MSCI failure is*

> *often associated with defective X-Y pairing. This could be easily addressed by examination of their RNAseq data.*

To address the concern that *Znhit1* deletion may impact Meiotic Sex Chromosome Inactivation (MSCI), we analyzed XY-linked gene expression using scRNA-seq data from spermatocytes at distinct stages. Our analysis revealed aberrant activation of XY-linked genes in *Znhit1*-CKO spermatocytes relative to controls. Specifically, 120 XY-linked genes were activated at zygotene, and 119 XY-linked genes were upregulated at pachytene (revised Fig. 4F). This observation directly demonstrates that *Znhit1*-CKO impairs MSCI, which aligns with our prior characterization of defective X-Y chromosome synapsis in *Znhit1*-deficient spermatocytes. To explicitly resolve this concern, we have integrated these MSCIfocused RNA-seq analyses into the revised Results section (lines 221-226).

> *(3) The recombination assays need attention.*
>
> *In the text the authors state that they studied RPA2 and DMC1, but the figures show RPA2 and RAD51.*
>
> *The RPA counts are not quantitated.*
>
> *The conclusion that crossover formation fails (based on MLH1 staining) is not justified. This marker does not appear in wt males until late pachytene, so if cells in this mutant are dying before that stage, MLH1 cannot be assessed.*
>
> *The authors state that gH2AZ persists in the KO, but I'm not convinced that they are comparing equivalent stages in the wt and KO. In Figure 3C, the pachytene cell is late, whereas in the mutant the pachytene cell is early or mid (when residual gH2AX is expected, even in wt males).*
>
> *Previous work (PMID: 23824539) has shown that antibodies reportedly detecting pATM in the sex body are non-specific. I therefore advise caution with the data shown in Figure 3D.*

We appreciate the reviewer's detailed feedback on our recombination assays and have addressed each concern as follows:

(1) Discrepancy between text and figures (RPA2/DMC1 vs. RPA2/RAD51): We have corrected this in the revised manuscript.

(2) Quantitation of RPA2 foci: We have supplemented quantitative analysis of RPA2 foci (revised Fig. S3).

(3) Conclusion on crossover failure: Single-cell RNA sequencing data from P35 testes definitively confirmed that *Znhit1* knockout spermatocytes successfully progressed to the late pachytene stage, ruling out the possibility that our MLH1 staining results are confounded by cell death or arrest before this critical stage. In addition, analysis of transcriptome datasets revealed significant downregulation of important genes required for homologous recombination and crossover formation, including *Ccnb1ip1* and *Rnf212*. Reduced expression of these essential factors may impair the assembly of MLH1 crossover foci. These data demonstrate that ZNHIT1 is essential for proper homologous recombination and crossover formation during male meiosis. We have revised the text to emphasize this context.

(4) γH2AX persistence and stage matching: We have replaced the images with more representative, stage-matched pachytene spermatocytes from wild-type and *Znhit1*-KO mice (revised Fig. 2C). Furthermore, prompted by the insightful comment from Reviewer 1, we carefully re-examined autosomal synapsis and identified abnormal synapsis specifically at the terminal regions of autosomes in *Znhit1*-deficient spermatocytes (revised Fig. 3A). These data together confirm that ZNHIT1 is essential for DSB repair during male meiotic prophase I.

(5) pATM staining issue: Following the reviewer's advice, we carefully reviewed the relevant literature (PMID: 23824539) and confirmed that the anti-pATM antibody may exhibit non-specific staining on the XY chromosomes. Accordingly, we have removed the pATM staining data presented in Figure 3D from the revised manuscript to ensure the accuracy and rigor of our results.

> *(4) RNAseq data. The authors show convincingly that Znhit1 activates genes that are normally upregulated at the zyg-pachytene transition. They should repeat the analysis for genes normally upregulated at the prelep- lep and lep-zyg transition to show that this effect is really pachytene-gene specific.*

We appreciate this suggestion. To clarify the stage specificity of ZNHIT1's regulatory role, we analyzed genes upregulated at the prelep-lep and lepzyg transitions. Our results showed that *Znhit1* knockout had little impact on the overall expression levels of these genes (as shown in revised Fig. 4B). In contrast, as we previously reported, genes upregulated at the zygotene-pachytene transition were remarkably downregulated in *Znhit1*-cKO. These findings further confirm the specificity of ZNHIT1 in regulating pachytene gene expression.

> *(5) I am puzzled that the title and overall gist of the study focuses on H2A.Z, when it is Znhit1 that has been deleted.*

We appreciate the reviewer's observation and have revised the study title as suggested. Specifically, the title is now updated to "ZNHIT1-dependent H2A.Z deposition at meiotic prophase I underlies pachytene gene expression and meiotic progression during male meiosis."

> ***Reviewer #3 (Public Review):***
>
> *Summary:*
>
> *Sun et al. present a manuscript detailing the phenotypic characterization of loss of Znhit1 in male germ cells. Znhit1 is a subunit of the chromatin regulating complex SRCAP that functions to deposit the histone variant H2A.Z. Given that meiosis, and specifically meiotic recombination, occurs in the context of the dynamic condensing of chromosomes, the role of chromatin regulators in general, and histone variants specifically, in mammalian meiosis is an active area of research. Previous work has shown that H2A.Z is found at the locations of recombination in plants, although H2A.Z was previously not found at recombination sites in mammalian meiosis. Here the authors use a conditional approach to ablate Znhit1 in spermatocytes and characterize a block in meiosis in prophase I in the transition from pachytene to diplotene stage.*
>
> *Strengths:*
>
> *The authors combine current methods in immunohistochemistry and functional genomics to provide strong evidence of meiotic block upon the loss of Znhit1. They find that loss of Znhit1 leads to reduced incorporation of the histone variant H2A.Z, specifically at promoters and enhancers. Further, RNA sequencing found more genes are down-regulated upon loss of Znhit1 compared to upregulated, suggesting that*

> *incorporation of H2A.Z is critical for the expression of genes necessary for successful meiotic progression.*
>
> *A strength of the manuscript is tying the locations of changes in H2A.Z deposition with binding of the transcription factor A-MYB, providing a mechanism that can potentially combine the changes in chromatin regulation with variable binding of a transcription factor in gene expression in pachytene stage spermatocytes.*
>
> *Weaknesses:*
>
> *A weakness in the single-cell RNA experiment using cells from 16-day-old male mice. The authors suggest that the rationale for the experiment was to determine where the Znhit1-sKO mutant showed an arrest in meiosis, and claim that this is the pachytene stage. However, in the 'first wave' of meiosis 16-day-old mice are just beginning to enter pachytene, so cells from later meiotic stages will be largely absent in these tubules. This is clear from the UMAP showing a similar pattern of cell distributions between wild-type and mutant mice. Using older mice would have better demonstrated where the mutant and wild-type mice differ in cell-type composition.*

We appreciate the reviewer's constructive comment. To resolve this issue, we have added new scRNA-seq data from testes of P35 mice, which harbor a full spectrum of meiotic stages, including late pachytene, diplotene, metaphase I spermatocytes, and post-meiotic spermatids. Compared with wild-type controls, *Znhit1*-sKO testes exhibited a marked reduction in late pachytene spermatocytes and a near-complete loss of post-pachytene cell types, directly validating the pachytenestage meiotic arrest (revised Fig. 2F, G). All updated analyses have been integrated into the manuscript to strengthen our conclusions.

> *The authors use the term pachytene genome activation (PGS) in the manuscript to suggest a novel process by which genes are specifically increased in expression in the pachytene stage of meiotic prophase I, without reference to literature that establishes the term. If the authors are putting forward a new concept defined by this term, it would strengthen the manuscript to describe it further and delineate what the genes are that are activated and discuss potential mechanisms.*

We appreciate the reviewer's valuable feedback on our use of the term "pachytene genome activation (PGA)".

To address this, we have revised the text to explicitly frame PGA as a stage-specific transcriptional program observed in our data, defined by the coordinated upregulation of a distinct set of genes during the pachytene stage of meiotic prophase I.

(1) Definition and Gene Set: Using the scRNA-seq dataset, we formally defined PGA as the transcriptional wave characterized by genes with increased expression in pachytene vs. zygotene spermatocytes (n = 1,560 genes). Functional enrichment analysis shows these genes are primarily involved in DNA repair, cilium organization, and spermatid development (Table S3), consistent with the biological process of germ cell development.

(2) Relationship to existing literature: While PGA as a term is not widely established, our data align with prior observations of pachytene-specific transcriptional upregulation (Alexander et al., 2023; Ernst et al., 2019; Turner, 2015). Importantly, Alexander et al reveals that in late meiotic stages, starting from pachynema, chromatin has a ~3-fold increase in transcription. We have added these citations to clearly illustrate the relevant advances in the field (lines 68-71).

(3) Regulation of pachytene-stage gene expression: We further delineate that PGA is regulated by ZNHIT1-dependent H2A.Z deposition. *Znhit1* deletion resulted in significant downregulation of 70.1% (1,094 out of 1,560) of these genes. This links PGA to chromatin-

based regulation, where ZNHIT1-dependent H2A.Z deposition enables pachytene-specific transcription.

> *Generally speaking, the authors present solid evidence for a pachytene block in male germ cell development in mice lacking Znhit1 in spermatocytes. The evidence supporting a change in gene expression during pachytene, that more genes are downregulated in the mutant compared to increased expression, and changes in histone modification dynamics and placement of H2A.Z all support a role in alterations in meiotic gene regulation. However, the support that changes in H2A.Z impacting meiotic recombination (as suggested in the manuscript title) is less supported, rather than a general cell arrest in the pachytene stage leading to cell death. The conclusions around the role of Znhit1 influencing meiotic recombination directly could use further justification or mechanistic hypothesis.*

We acknowledge the reviewer's comments. Indeed, existing data support the presence of a pachytene block in spermatocytes of *Znhit1*-deficient mice, along with aberrant pachytene gene expression and impaired H2A.Z deposition.

In response, we made the following revisions: (1) we adjusted the manuscript title and conclusion to reduce emphasis on a direct H2A.Z-recombination link, and focus instead on ZNHIT1/H2A.Z in pachytene gene regulation and meiotic progression; (2) recombination defects may be indirect consequences of failed pachytene gene regulation, rather than a direct regulatory effect of ZNHIT1 on recombination machinery (lines 314-319).

> ***Reviewer #3 (Recommendations For The Authors):***
>
> *Quality of the images for meiotic spreads - images have low contrast and are tiny. It is difficult to see the SYCP3 results even when the images are magnified on the computer screen.*

We have provided new images with high resolution to ensure a clear visualization of SYCP3 signals.

> *Line 165 - indicates the results for DMC1, although the figure suggests the results are for RAD51 foci.*

We have corrected this mistake.

> *Line 306 - this manuscript 'confirms' that H2AZ is not found at mammalian recombination sites, a result already in the literature.*

We have corrected this mistake (lines 309-312).

> ***Reviewing Editor Comments:***
>
> *Major points and revisions highlighted by the reviewers:*
>
> *(1) Meiotic prophase in Znhit1KO: The main questions to clarify are the stage and status of progression, the analysis of apoptosis, and the consequences of gene expression on the X and Y. Additional analysis for DSB repair foci, gH2AX is also required. Those analysis are needed to answer to reviewer 2. Even if H2AZ was not detected at recombination hotspots, it may be possible that it plays a role in DSB repair but the level is too low for detection. This should be discussed as H2AZ was shown to be involved in DNA repair.*

We sincerely appreciate the reviewing editor's constructive comments.

(1) Stage and progression of meiotic prophase: We supplement P35 testes for scRNAseq. Results confirmed *Znhit1*-KO spermatocytes arrest at late pachytene, and postpachytene

stages (diplotene, metaphase I) were nearly absent (revised Fig. 2F, G).

(2) Apoptosis analysis: We studied this by demonstrating that apoptosis-related genes were upregulated in pachytene spermatocytes at the single-cell level (revised Fig. 4D). To further validate this finding, we performed scRNA-seq analysis on P35 testis samples. Our results revealed a marked reduction in late pachytene spermatocytes in *Znhit1*-cKO testes (revised Fig. 2F, G), consistent with apoptotic depletion of pachytene-stage cells. Together, these data confirm that *Znhit1* ablation impairs pachytene-stage spermatocyte development.

(3) X/Y gene expression consequences: To address this key point, we performed stage-resolved analysis of XY-linked gene expression using scRNA-seq data from different-stage spermatocytes. Compared with controls, we detected aberrant ectopic activation of XY-linked genes in *Znhit1*-KO spermatocytes: 120 XY-linked genes were inappropriately activated at zygotene, and 119 remained abnormally upregulated at pachytene (revised Fig. 4F). These results provide direct evidence that *Znhit1* deletion impairs Meiotic Sex Chromosome Inactivation (MSCI).

(4) DSB repair issue: We have replaced the images with more representative, stage-matched pachytene spermatocytes (revised Fig. 3C). The revised images show consistently increased γH2AX signals in *Znhit1*-KO spermatocytes. Prompted by Reviewer 1's comment, we identified abnormal synapsis at autosomal terminal regions in mutant cells. Together, these results confirm that ZNHIT1 is essential for DSB repair during male meiotic prophase I.

(5) Potential role of H2A.Z in DSB repair: Though H2A.Z was nearly undetectable at recombination hotspots, we discuss two possibilities: (1) ZNHIT1-H2A.Z depletion dysregulated DSB repair-related genes; (2) Current ChIP-seq sensitivity may miss low-abundance H2A.Z at hotspots, which could support repair via chromatin remodeling. Future high-resolution assays (super-resolution imaging, DSB-targeted ChIP-seq) are proposed to validate this. We agree that recombination defects may be indirect consequences of failed pachytene gene regulation, rather than a direct regulatory effect of ZNHIT1 on recombination machinery.

> *(2) Gene expression analysis. The first consequence of H2AZ depletion is gene expression downregulation. However, it may be not surprising that some genes are down and others upregulated. There are likely secondary and indirect effects including the upregulation of some genes. The authors should explain and discuss this point such as to answer to questions raised by reviewer 1 and 2.*

The primary consequence of H2A.Z depletion in pachytene spermatocytes is indeed widespread downregulation of genes. For the coexistence of upregulated genes, we explain this via three key points.

(1) Technical differences between scRNA-seq and bulk RNA-seq (addressing Reviewer 1): scRNA-seq captures cell-type-specific differentially expressed genes that bulk RNA-seq masks (bulk averages signals across mixed cells, hiding changes in rare subsets). Additionally, scRNA-seq uses a lower log2(fold change) threshold (0.25 vs. 1 in bulk RNA-seq), detecting subtle upregulations missed by bulk analysis.

(2) No dead cell contamination (addressing Reviewer 1): Stringent quality control excluded cells with >15% mitochondrial RNA. Apoptosis-related genes showed no significant correlation with mitochondrial RNA fractions (Pearson correlation coefficient, r = -0.02; please see Author response image 1), ruling out dead cell transcriptome interference.

(3) Secondary/indirect effects (addressing Reviewers 1 & 2): Upregulated genes likely result from indirect regulatory cascades. H2AZ depletion may disrupt upstream transcription factors, leading to compensatory upregulation of their downstream genes or cell stress responses to meiotic arrest. Notably, *Znhit1* knockout specifically impacts genes upregulated

at the zygotene-pachytene transition, while genes upregulated at preleptotene-leptotene or leptotene-zygotene transitions remain largely unaffected (revised Fig. 4B), confirming the specificity of H2A.Z's direct regulatory role and framing upregulation as non-targeted indirect effects.

> *(3) The authors should also test the effect of Znhit1KO on the 1196 genes (up PreL/L) and 1325 (up L/Z) as shown in Figure 5D for the PGA. Also in Figure 5B, there is no evaluation of the statistical significance of the variation, this should be revised. X and Y genes should be analysed. KAS-Seq should be correlated with gene expression analysis, and several points as mentioned in the reviews below should be better explained and discussed.*

(1) Effect of *Znhit1*-KO on PreL/L- and L/Z-upregulated genes: we analyzed the 1196 genes upregulated at the PreL/L transition and 1325 genes upregulated at the L/Z transition. *Znhit1* knockout had minimal effect on the expression of these early meiotic gene sets (revised Fig. 4B), whereas genes activated at the zygotene-pachytene transition were strongly downregulated in *Znhit1*-KO spermatocytes. These results confirm the specific role of ZNHIT1 in regulating pachytene-stage gene expression. We have also added a statistical evaluation for the variation shown in Fig. 4B.

(2) X/Y-linked gene analysis: Analysis of stage-resolved scRNA-seq revealed aberrant ectopic activation of 120 XY-linked genes at zygotene and 119 at pachytene in *Znhit1*-KO spermatocytes (revised Fig. 4F), demonstrating impaired Meiotic Sex Chromosome Inactivation (MSCI).

(3) KAS-seq correlation with gene expression: We analyzed the link between KAS-seq signals and gene expression, and we found that *Znhit1* depletion caused a global reduction in KAS-seq signals, especially at promoters of downregulated genes (revised Fig. S8). Genes with increased expression showed low KAS-seq signals in both control and mutant groups, likely reflecting indirect regulation. These results highlight the essential role of ZNHIT1 in transcriptional regulation.

> *(4) The title should refer to Znhit1, and the effect on meiotic recombination activities may be an indirect consequence of prophase progression arrest, even if some recombination genes are downregulated. This point is important as noted by reviewer 3.*

We fully acknowledge Reviewer 3's key point and have revised the manuscript title to "ZNHIT1-dependent H2A.Z deposition at meiotic prophase I underlies pachytene gene expression and meiotic progression during male meiosis" to reduce emphasis on a direct H2A.Z-recombination link.

Regarding meiotic recombination activities: The downregulation of recombinationrelated genes (e.g., *Ccnb1ip1*, *Rnf212*) stems from impaired pachytene-stage transcriptional programs caused by ZNHIT1-dependent H2A.Z deposition defects, which in turn leads to prophase progression arrest. Thus, the observed recombination abnormalities may be a secondary consequence of the meiotic prophase arrest, rather than a direct regulatory effect of ZNHIT1 on recombination machinery. This clarification has been integrated into the Discussion section (lines 314-318).

> *(5) The recent structural analysis of SRCAP should be cited: Yu et al. Cell Discovery (2024) 10:15 https://doi.org/10.1038/s41421-023-00640-1.*

We have cited this reference in this revised manuscript (lines 234-236).

> *(6) The authors should read and answer the specific revisions asked for by the reviewers.*

We have thoroughly read and systematically addressed all specific revisions requested by Reviewers 1, 2, and 3, as detailed in the revised manuscript and supplementary data.

References

Alexander, A.K., Rice, E.J., Lujic, J., Simon, L.E., Tanis, S., Barshad, G., Zhu, L., Lama, J., Cohen, P.E., and Danko, C.G. (2023). A-MYB and BRDT-dependent RNA Polymerase II pause release orchestrates transcriptional regulation in mammalian meiosis. Nature communications 14.

Cole, L., Kurscheid, S., Nekrasov, M., Domaschenz, R., Vera, D.L., Dennis, J.H., and Tremethick, D.J. (2021). Multiple roles of H2A.Z in regulating promoter chromatin architecture in human cells. Nature communications 12, 2524.

Ernst, C., Eling, N., Martinez-Jimenez, C.P., Marioni, J.C., and Odom, D.T. (2019). Staged developmental mapping and X chromosome transcriptional dynamics during mouse spermatogenesis. Nature communications 10, 1251.

Kim, T.K., Hemberg, M., Gray, J.M., Costa, A.M., Bear, D.M., Wu, J., Harmin, D.A., Laptewicz, M., Barbara-Haley, K., Kuersten, S., et al. (2010). Widespread transcription at neuronal activity-regulated enhancers. Nature 465, 182-187.

Sporrij, A., Choudhuri, A., Prasad, M., Muhire, B., Fast, E.M., Manning, M.E., Weiss, J.D., Koh, M., Yang, S., Kingston, R.E., et al. (2023). PGE(2) alters chromatin through H2A.Z-variant enhancer nucleosome modification to promote hematopoietic stem cell fate. Proceedings of the National Academy of Sciences of the United States of America 120, e2220613120.

Turner, J.M. (2015). Meiotic Silencing in Mammals. Annu Rev Genet 49, 395-412. Wu, T., Lyu, R., You, Q., and He, C. (2020). Kethoxal-assisted single-stranded DNA sequencing captures global transcription dynamics and enhancer activity in situ.

Nature methods 17, 515-523.

https://doi.org/10.7554/eLife.99713.2.sa0